# Nitrite-Mediated Photooxidation of Vanillin in Atmospheric Aqueous

2	Phase
3	
4 5 6	Hongwei Pang <sup>1</sup> , Qi Zhang <sup>2</sup> , Xiaohui Lu <sup>1</sup> , Kangning Li <sup>1</sup> , Hong Chen <sup>1</sup> , Jianmin Chen <sup>1</sup> Xin Yang <sup>1,3</sup> *, Yingge Ma <sup>4</sup> , Jialiang Ma <sup>4</sup> , Cheng Huang <sup>4</sup>
7 8 9	<sup>1</sup> Shanghai Key Laboratory of Atmospheric Particle Pollution and Prevention Department of Environmental Science and Engineering, Fudan University, Shangha 200433, China
10	<sup>2</sup> Department of Environmental Toxicology, University of California, Davis, California
11	95616, United States
12	<sup>3</sup> Shanghai Institute of Pollution Control and Ecological Security, Shanghai 200092
13	China
<ul><li>14</li><li>15</li><li>16</li></ul>	<sup>4</sup> State Environmental Protection Key Laboratory of Formation and Prevention of th Urban Air Pollution Complex, Shanghai Academy of Environmental Sciences Shanghai 200233, China
17	
18	Correspondence to: yangxin@fudan.edu.cn
19	
20	
21	
22	
23	
24	
25	
26	
27	
28	
29	
30	
31	
32	
33	

Abstract: Nitrite (NO<sub>2</sub>), and its conjugate acid nitrous acid (HNO<sub>2</sub>), has long been recognized as a ubiquitous atmospheric pollutant as well as an important photochemical source of hydroxyl radical (•OH) and reactive nitrogen species (•NO, •NO<sub>2</sub> and •N<sub>2</sub>O<sub>3</sub>, etc.) in both gas phase and aqueous phase. Although NO<sub>2</sub> /HNO<sub>2</sub> plays an important role in atmospheric chemistry, our understanding on its role in the chemical evolution of organic components in atmospheric waters is rather incomplete and is still in dispute. In this study, the nitrite-mediated photooxidation of vanillin (VL), a phenolic compound abundant in biomass burning emissions, was investigated under pH conditions relevant for atmospheric waters. The influence of solution pH, dissolved oxygen and •OH scavenger on the nitrite-mediated photooxidation of VL was discussed in detail. Our study reveals that the molecular composition of the products is dependent on the molar ratio of NO<sub>2</sub>/VL in the solution and that nitrophenols are the major reaction products. We also found that the light absorbance of the oxidative products increases with increasing pH in the visible region, which can be attributed to the deprotonation of the nitrophenols formed. These results contribute to a better understanding of methoxyphenol photooxidation mediated by nitrite as a source of toxic nitrophenols and climatically important brown carbon (BrC) in atmospheric waters.

#### 1. Introduction:

Aromatic compounds, emitted from both anthropogenic (e.g., fuel burning) and natural (e.g., wild fire) processes, are ubiquitous in the polluted troposphere. They account for as much as 50% of the non-methane hydrocarbon mass in urban air¹ and are known to contribute substantially to the formation of secondary organic aerosol (SOA), which has huge impacts on climate, human health and air quality.², ³ The oxidation of aromatic compound often occurs by adding polar oxygenated functional group to the aromatic ring, which decreases its volatility and increases its water solubility.⁴ Subsequently, the semivolatile, oxidized aromatic compounds can partition between gaseous and condensed phases and undergo transformation in different environments. There is a growing understanding that tropospheric aqueous-phase reactions play an important role in the chemical evolution of semivolatile organics under atmospherically relevant conditions.³, ⁵ It is well known that atmospheric droplets (i.e., in clouds and fogs) provide an liquid water medium for aqueous-phase chemistry to take place.⁵ In addition, aqueous aerosols are the medium for homogeneous as well as heterogeneous chemistry.

Phenols are a class of aromatic compounds that have at least one hydroxyl (-OH) group bonded directly to an aromatic ring. Phenols are potentially harmful to human health and the environment.<sup>6</sup> In addition, phenols are important precursors that contribute to SOA formation, including brown carbon (BrC).<sup>7-9</sup> Phenolic compounds can be emitted directly into the atmosphere by biomass and fossil fuel burning<sup>10</sup> or be formed *in situ* as products of atmospheric oxidation of aromatic hydrocarbons.<sup>11, 12</sup> The atmospheric transformations of phenols can take place in both the gas and aqueous phases.<sup>13-15</sup> The gas-phase oxidation of phenolic compounds has been shown to be initiated mainly by the reactions with OH and NO<sub>3</sub> with O<sub>3</sub> playing a negligible role.<sup>6, 16-18</sup> Recent studies have shown that phenols can react rapidly in atmospheric aqueous phases and form aqSOA (SOA formed through aqueous-phase reactions) with high mass yields.<sup>13, 14, 19</sup> However, the detailed mechanisms on aqueous oxidation of phenols remains unclear. A key factor in directing the aging of phenols in aqueous phase is the availability of oxidants, such as hydroxyl radical,<sup>9</sup> triplet excited states of

organic matter (<sup>3</sup>C\*) <sup>13, 14</sup> and reactive nitrogen species (RNS). <sup>20, 21</sup> Compared to the •OH- or <sup>3</sup>C\*- mediated oxidation of phenols, there are very few studies on the aqueous-phase oxidative aging of phenols mediated by RNS. Field studies have observed that nitrophenols (NPs) are ubiquitous in cloud, fog and rainwater and that their concentrations are significantly higher than might be expected from direct emissions from combustion and fertilization processes. <sup>22</sup> These observations suggest that aqueous-phase reactions of phenols with RNS may be an important secondary source of nitrophenols. Nitrophenols are toxic and have attracted attention for their toxicity on human health and other living organisms. <sup>23, 24</sup> Moreover, nitrophenols are a well-known light absorber, thus can exert positive effects on atmospheric radiative forcing. <sup>25-27</sup>

N<sub>2</sub>O<sub>5</sub>, ClNO<sub>2</sub>, NO<sub>2</sub>-/HNO<sub>2</sub> and HOONO, being recognized as sources of RNS (NO<sup>+</sup>, NO<sub>2</sub><sup>+</sup>, NO and NO<sub>2</sub>), are powerful nitrating agents of aromatic compounds in atmospheric waters. <sup>28-31</sup> Once partition into the aqueous phase, N<sub>2</sub>O<sub>5</sub> and ClNO<sub>2</sub> can hydrolyze to form the nitronium ion NO<sub>2</sub><sup>+</sup>, <sup>32</sup>, <sup>33</sup> a nitration electrophile which plays an important role in the dark nitration of phenols. Depending on the level of pollution, the concentration of NO<sub>2</sub>-/HNO<sub>2</sub> in cloud waters can range from 0.01 to 1000 µM.<sup>34</sup> NO<sub>2</sub>-/HNO<sub>2</sub> (i.e., N(III)) is an important source of RNS both in the dark and under illumination. 35-38 As shown in Table 1, HNO<sub>2</sub> can produces NO<sup>+</sup>, •NO and •NO<sub>2</sub> upon protonation and thermal degradation in the dark (reactions 1 and 2). 38, 39 In addition, HNO<sub>2</sub> can react with H<sub>2</sub>O<sub>2</sub> to form peroxynitrous acid (HOONO) (reaction 3),<sup>31</sup> which is a powerful nitrating agent and an important intermediate in atmospheric chemistry. 40 HOONO is unstable in aqueous solution and quickly isomerizes to HNO<sub>3</sub> or decomposes to form •OH and •NO<sub>2</sub> (reaction 4).<sup>29, 41</sup> The photolysis of nitrite and nitrous acid mainly produces •OH, •NO and •NO2 (reactions 5-9).40, 42, 43 The generation of •OH by nitrite photolysis is pH-dependent, as shown in reaction 6. However, since the protonation of •O is very fast in aqueous solution at pH <12, 44 pH has a negligible influence on the •O<sup>-</sup>/•OH equilibrium in atmospherically relevant pH range (0~9). 8, 67 In addition to being a source of •OH, NO<sub>2</sub>-/HNO<sub>2</sub> can also be oxidized by •OH to form •NO<sub>2</sub> (reactions 7 and 9).

The photoreactions between NO<sub>2</sub>/HNO<sub>2</sub> and phenols may represent an important sink for phenolic compounds in atmospheric waters.<sup>22</sup> However, the mechanisms by which phenols react with NO<sub>2</sub>-/HNO<sub>2</sub> in aqueous phase are still unclear. For example, there have been questions regarding the influences of key factors such as pH, O<sub>2</sub>, and • OH scavenger on the NO<sub>2</sub>/HNO<sub>2</sub>-mediated photooxidation of phenols. The influence of the molar ratio of NO<sub>2</sub>/phenols on the molecular composition of the photooxidative products also needs to be clarified. In this work, we focus on the photooxidation of vanillin (VL) by NO<sub>2</sub>-/HNO<sub>2</sub> in aqueous solutions under atmospherically relevant pH conditions. Vanillin is chosen as a model compound of methoxy-phenols which are abundant in biomass burning emissions. 10, 45 Since vanillin has an intermediate volatility (approximately 10<sup>3</sup> μg m<sup>-3</sup>) <sup>46</sup> and a high Henry's constant  $(4.56 \times 10^5 \text{ M atm}^{-1} \text{ at } 298\text{K})$ , <sup>47</sup> aqueous-phase reactions are likely an important oxidation pathway for it in the atmosphere. This work is the first to present comprehensive kinetic and mechanistic information on the photooxidation of vanillin by NO<sub>2</sub>7/HNO<sub>2</sub> under conditions relevant to atmospheric droplets. The effects of pH, dissolved oxygen, and •OH scavenger on the photooxidation of VL were investigated. The reaction products were identified by high-resolution mass spectrometry (HRMS) coupled with ultrahigh performance liquid chromatography (UPLC). In addition, we systematically examine the pH-dependent light absorbance of the nitrophenol products and provide explanations for the link between pH and observed absorption. Our results indicate that nitrite chemistry plays a significant role in the formation of aqueous nitrated aromatics, which can potentially influence radiative forcing as well as human health.

147

148

149

150

151

152

123

124

125

126

127

128

129

130

131

132

133

134

135

136

137

138

139

140

141

142

143

144

145

146

# 2. Experimental section:

All photochemical experiments were performed in a 200ml, airtight Pyrex tube (completely blocking light below 285 nm) equipped with a magnetic stirrer and a bubble tube for feeding high-purity air or nitrogen. The Pyrex tube containing solution was illuminated inside a RPR-200 photoreactor (New England Ultraviolet

Company) equipped with 300, 350, 419 nm bulbs (2, 7, and 7 bulbs, respectively) to mimic sunlight. 48 Except where noted, the photochemical reactions were performed under the following experimental conditions:  $[VL]_0 = 0.1 \text{ mM}$  and  $[NaNO_2]_0 = 1 \text{ mM}$ at the solution pH 5.0 with 100 mL air-saturated solution. The 10:1 molar ratio of NO<sub>2</sub>-vanillin (i.e., 1 mM NaNO<sub>2</sub> and 0.1 mM VL) used may reflect the concentration ratio of NO<sub>2</sub> and VL found in atmospheric waters in highly polluted urban locations where the concentration of  $NO_x$  is high. At pH = 5.0, 98.6% N(III) is presents as  $NO_2$ (Figure S1). NO<sub>2</sub> reacts rapidly with •OH to produce •NO<sub>2</sub> through one-electron oxidation (reaction 7). The second-order rate constant for the reaction between •OH and  $NO_2^-$  (k = 1.0 × 10<sup>10</sup> M<sup>-1</sup> s<sup>-1</sup>)<sup>35</sup> is 25 times larger than that for the reaction between •OH and VL ( $k = 4 \times 10^8 \text{ M}^{-1} \text{ s}^{-1}$ ). According to the kinetic calculation (1) presented in SI, for 10:1 molar ratio of NO<sub>2</sub> to VL, 99.6% of the photoformed •OH would react with NO<sub>2</sub> to generate •NO<sub>2</sub> and only the remaining 0.4% reacts with VL. As a result, in the solution with pH = 5.0 and NO<sub>2</sub>/VL molar ratio = 10:1, nitrite acts primarily as a source of •NO<sub>2</sub> rather than •OH. The materials, reagents and additional experimental details are provided in the Supporting Information.

The concentrations of VL, 5-nitrovanillin (5NV) and 4-nitroguaiacol (4NG) were determined by HPLC. The experimental error in the HPLC measurements is < 2% according to triplicate runs. The oxidation products of VL were analyzed and formula-assigned by an Orbitrap HRMS (mass resolution m/Δm =140,000) equipped with an electrospray ionization (ESI) source and an UPLC. The light absorptivity of the solutions was measured by UV-vis spectroscopy. Gas chromatography/mass spectrometry (GC-MS) was applied to identify the molecular structure of the main nitration products. All speciation calculations in this work were carried out with a chemical equilibrium calculation program - Visual MINTEQ (developed by KTH, SEED, Stockholm, Sweden). Details on the analytical procedures are given in the Supporting Information.

## 3. Results and discussion

# 3.1 Nitrite-mediated photooxidation kinetics of vanillin (VL) in aqueous phase

Under simulated sunlight illumination, VL was found to undergo rapid oxidation in the presence of nitrite and the reaction rates were found to be strongly dependent on solution pH, the availability of dissolved O<sub>2</sub> and •OH scavenger. As shown in Figure 1, the two most abundant first-generation products of VL photooxidation are 5-nitrovanillin (5NV) and 4-nitroguaiacol (4NG). Next we elucidate the effects of pH, dissolved O<sub>2</sub> and •OH scavenger on the nitrite-mediated aging processes of VL based on the kinetics of VL degradation and 4NG and 5NV formation.

191

192

193

194

195

196

197

198

199

200

201

202

203

204

205

206

207

208

209

210

211

212

183

184

185

186

187

188

189

190

## 3.1.1 Influence of pH

The pH values observed in atmospheric water droplets and aqueous aerosol particles were frequently found to be in range of 3 to 5,49,50 so we investigated the effects of pH on the photooxidation of VL under simulated sunlight irradiation by conducting experiments on the air-saturated solutions of 1mM NO<sub>2</sub> and 100 µM VL with pH adjusted to 3 to 5. As shown in Figure 2a and Figure S2, the photodegradation of VL  $(pK_a = 7.9)^{51}$  followed pseudo-first order kinetics and the decay rate was faster under more acidic conditions. For instance, the rate constant is more than a factor of 3 higher at pH = 3 ( $2.3 \times 10^{-2} \text{ min}^{-1}$ ) than at pH = 5 ( $7.1 \times 10^{-3}$ min<sup>-1</sup>; Figure S2). The observed pH effect can be attributed to the dependence of N(III) speciation on solution acidity. The pKa of HNO<sub>2</sub> is 3.2,<sup>36</sup> above which nitrite (NO<sub>2</sub>), the deprotonated counterpart of HNO<sub>2</sub>, becomes the dominant N(III) species (Figure S1). The photolysis quantum yield of HNO<sub>2</sub> is higher than that of NO<sub>2</sub> in the near-UV region. 43, 52 Thus, as pH decreases, the •OH formation rate in the illuminated N(III) solution increases, resulting in a faster degradation rate of VL. Note that although the direct photodegradation rate of VL in aqueous phase is also likely pH dependent, this rate is much slower than the photoreaction rate between N(III) and VL (Figure 2a). Figure S3 shows the concentration vs. time curves for the nitrophenol products

(e.g., 5NV and 4NG) at different pH values. Both the formation and transformation

at different pH values are shown in Figure S4a-c. The absolute value of the slope for the line represents the yield of 5NV or 4NG. For example, at pH 3.0, the yields of 5NV and 4NG were 51% and 24%, respectively. However, as the kinetics was fast at pH 3.0, the yields of nitrophenol can be calculated only over initial 2 data points with larger uncertainties (Figure S4a). In contrast, the yields of 5NV and 4NG can be determined more precisely at pH 4.0 and 5.0. The yields for 5NV and 4NG were (33  $\pm$ 1)% and 16% at pH 4.0 (Figure S4b) and 43% and 20% at pH 5.0 (Figure S4c). Apparently, almost no lesss than half of the VL reacted was transformed into 5NV and 4NG at different pH values. 

Dark control experiments were also performed to investigate the reactivity of N(III) towards VL. As shown in Figure S5a and b, no degradation of VL was observed at pH 5.0 in the air-saturated solutions of 1mM NO<sub>2</sub><sup>-</sup> and 100  $\mu$ M VL kept in the dark and the pseudo-first-order rate constants for VL decay at pH 3.0 and 4.0 (1.0  $\times$  10<sup>-3</sup> min<sup>-1</sup> and 9.3 $\times$  10<sup>-5</sup> min<sup>-1</sup>, respectively) were much lower than the corresponding VL photooxidation rate constants (2.3  $\times$  10<sup>-2</sup> min<sup>-1</sup> and 8.5 $\times$  10<sup>-3</sup> min<sup>-1</sup> at pH 3.0 and 4.0, respectively; Figure S2). These results indicate that dark reactions have a minor influence on the results of photooxidation kinetics.

# 3.1.2 Influence of dissolved O<sub>2</sub>

Several studies have reported that  $O_2$  can exert positive effects on N(III)-mediated photooxidation of organic and inorganic species.<sup>30, 43</sup> However, a mechanistic understanding on how  $O_2$  influences the photooxidation of phenols is still lacking. We thus examined the effect of dissolved oxygen on the N(III)-mediated photooxidation of VL in this study by conducting experiments on the air- or nitrogen-saturated solutions containing 1mM  $NO_2^-$  and 100  $\mu$ M VL with pH adjusted to 5.0. In our system, where  $NO_2^-$ /VL molar ratio = 10:1 (i.e.,  $1 \times 10^{-3}$  M vs.  $1 \times 10^{-4}$  M) and pH = 5, nitrite acts primarily as a source of  ${}^{\bullet}NO_2$  rather than  ${}^{\bullet}OH$ , as detailed in the experimental section. Therefore,  ${}^{\bullet}NO_2$  is the dominant reacting radical responsible for the oxidation of VL in solution.

As shown in Figure 2b, the rates for both VL photodegradation and 5NV and

4NG formation were significantly higher in air-saturated solution compared to those 243 in N<sub>2</sub>-saturated solution. For example, at the end of 180 min of illumination, nearly 73% 244 of the VL decayed under the air-saturated condition whereas only 13% decayed under 245 the N<sub>2</sub>-saturated condition. The molar yields for 5NV and 4NG were 43% and 20% in 246 air-saturated (Figure S4c) and  $(20 \pm 3)\%$  and  $(11 \pm 2)\%$  in N<sub>2</sub>-saturated (Figure S4d). 247 A possible reason for the faster VL degradation in O<sub>2</sub>-saturated solution is the 248 autoxidation of •NO in aqueous solution, 53-55 which opens up additional pathways for 249 forming •NO<sub>2</sub> (reactions 10 – 12 in Table 1). Specifically, the •NO stemming from 250 nitrite photolysis (reaction 5) can be rapidly oxidized by dissolved O2 to form ONOO 251 • - a weakly bound complex of •NO and O<sub>2</sub> (reaction 10). <sup>54</sup> ONOO• subsequently 252 interacts with another •NO to form an oxidizing intermediate ONOONO (reaction 253 11), the homolysis of which yields two •NO<sub>2</sub> (reaction 12). •NO<sub>2</sub> is an effective 254 nitrating agent whereas •NO is less reactive <sup>56</sup> and does not react with VL directly 255 (see details in 3.1.3). 256 Another possible explanation for the positive effect of O2 on VL reactions is 257 secondary photolysis of nitrite. Gligorovski et al. 57 proposed that the 258 photodissociation of NO<sub>2</sub><sup>-</sup> through reaction 13 can act as a minor reaction pathway to 259 produce  $\bullet NO_2$  and hydrated electron  $(e_{aq})$  with a low quantum yield of  $<10^{-3}$ . The 260 e<sub>aq</sub> is subsequently scavenged by dissolved O<sub>2</sub> accompanying the formation of a 261 superoxide radical anion (O2 • ) (reaction 14), which reacts with NO2 to yield • NO2 262 and H<sub>2</sub>O<sub>2</sub> (reaction 15)<sup>42</sup> or with •NO to form peroxynitrite (ONOO<sup>-</sup>) (reaction 16).<sup>41</sup> 263 Under typical conditions representative of acidic atmospheric water (e.g., pH=  $3\sim5$ ), <sup>58</sup> 264 ONOO undergoes protonation rapidly to form its conjugate acid, peroxynitrous acid 265 (HOONO)  $(pK_a = 6.8)^{59}$  (reaction 17), which homolyzes along the O-O bond to give 266 • NO<sub>2</sub> and • OH with a free radical yield of ca. 30% (reaction 4). 41 However, 267 accordingly to a study by Fischer and Warneck. <sup>36</sup>, there is no clear-cut experimental 268 evidence for or against the formation of eaq upon nitrite photolysis. Thus, the 269 pathway for the involvement of  $e_{aq}^-$  in VL nitration remains to be clarified. 270 Alternatively, VL may undergo photosensitized reactions and interact with O2 to form 271  $H_2O_2$  and  $O_2^{ullet}$ . 60 The photolysis of  $H_2O_2$  is a source of •OH. Both •OH and  $O_2^{ullet}$  can 272

react with NO<sub>2</sub><sup>-</sup> to form •NO<sub>2</sub> (reactions 7 and 15) and therefore promote the nitration of VL.

In addition, the photodegradation of VL plateaued after 60 min in the absence of O<sub>2</sub>, as shown in Figure 2b. This behavior may be attributed to the reverse of reaction 5 without O<sub>2</sub>. In the absence of O<sub>2</sub>, •NO may accumulate continuously in the solution due to the photolysis of NO<sub>2</sub>. The accumulation of •NO can result in a significant enhancement of the recombination reaction between •NO and •O<sup>-</sup>, thus inhibits the photolysis of NO<sub>2</sub> and concomitantly the photooxidation of VL. When the photolysis of NO<sub>2</sub> reaches chemical equilibrium with its reverse reaction (i.e., the recombination reaction between •NO and •O<sup>-</sup>), the photooxidation of VL stops and VL concentration reaches a plateau. The slight rise of VL concentration after 80 min (Figure 2b) was likely due to measurement uncertainties.

# 3.1.3 Influence of •OH scavenger

Atmospheric droplets contain a large number of organic and inorganic species, many of which may act as •OH scavengers  $^{61}$  and significantly inhibit •OH-induced nitration processes (reaction 7 and 9). In this work, the effect of •OH scavenger on the photonitration of VL was investigated by adding 500 mM 2-propanol (2P) to the air-bubbled solution containing 1mM NO<sub>2</sub> and 100  $\mu$ M VL at pH = 5.0. 2-propanol is an efficient •OH scavenger with a second order reaction rate constant of  $1.9 \times 10^9$  M $^{-1}$  s $^{-1}$ . $^{62}$  The reactions occur through H-abstraction by •OH to form (CH<sub>3</sub>)<sub>2</sub>COH•, which reacts with O<sub>2</sub> to produce acetone and HO<sub>2</sub>•(reactions 18-19; Table 1). $^{63}$ 

According to the kinetic calculation (2) presented in SI, the addition of 500 mM 2-propanol would cause 99% of •OH to react with 2-propanol, thus nearly completely inhibit the formation of •NO<sub>2</sub> through reaction 7. However, as shown in Figures 2c and S6, although 2-propanol indeed suppressed both the decomposition of VL and the formation of 5NV and 4NG, the impact was not as drastic. For example, in the system containing 500 mM 2-propanol, 46% of VL was degraded after 180 min of illumination, and the molar yields for 5NV and 4NG were 32% and 15%, respectively (Figure S4e). The results indicated that there were likely other pathways to produce

•NO<sub>2</sub>, in addition to the oxidation of NO<sub>2</sub><sup>-</sup> by •OH (reaction 7). One possible pathway is the oxidation of •NO by dissolved O<sub>2</sub> through reactions 10-12. Another possible pathway involves the aqueous reaction between •NO and HO<sub>2</sub>•, which forms HOONO (reaction 20) <sup>41</sup> and subsequently •OH and •NO<sub>2</sub> (reaction 4). Note that although •NO<sub>2</sub> can be formed through the photolysis of NO<sub>2</sub><sup>-</sup> (reaction 13), the quantum yield for this reaction is very low, thus the production of •NO<sub>2</sub> is likely negligible.

It is shown in Figure 2d that under N<sub>2</sub>-saturated conditions, no formation of 5NV or 4NG was observed in the photochemical system containing 1mM NO<sub>2</sub><sup>-</sup>, 100 μM VL and 500 mM 2-propanol at pH 5.0. This observation confirms the involvement of O<sub>2</sub> in the nitration of VL, such as oxidizing the •NO formed through reaction 5 to •NO<sub>2</sub> via reactions 10-12 or photosensitized reaction of VL as source of hydrogen peroxide (see discussions in section 3.1.2). Furthermore, the lack of nitrated products (e.g., 5NV and 4NG) suggests that •NO is too weak to react with VL.

# 3.2 The photooxidation pathways of VL in nitrite-containing solution

In order to elucidate the photooxidation mechanisms of VL in the presence of nitrite, we used HRMS coupled with a UPLC to investigate the molecular compositions of the reaction products. Figure 3a shows a chromatogram of the total ion current (TIC) of the solution mixture containing 10:1 molar ratio of  $NO_2^-/VL$  at pH 5 after 3 hours of photoreaction and Figure 3b shows the corresponding average negative mode ESI mass spectrum (MS) for compounds with retention times (RT) of 5-20 min. The chromatographic peak at 7.56 min RT corresponds to the reactant VL (m/z = 151.04011). Table S2 summarizes the RTs for the major reaction products and their molecular structures. A notable result is that no trimers or higher oligomers were detected in the products. However, a nitrated derivative of VL dimmer (m/z = 318.06195; peak 8 in Figure 3b) was tentatively detected in the products. In addition, both the primary nitration products, such as 5-nitrovanillic acid (m/z = 212.02011; peak 5), 5NV (m/z = 196.02487; peak 4) and 4NG (m/z = 168.03005; peak 2), and the second-generation nitration product 4,6-dinitroguaiacol (DNG) (m/z = 213.01522; peak 6) were detected. However, ions representing the product containing three or

more nitro groups were not detected in the HRMS. A possible reason is that the nitro group attached to the aromatic ring is electron-withdrawing and has a deactivating effect on the reactivity of the ring by making it electron deficient, thus prevents the addition of a third nitro group on the ring.

333

334

335

336

337

338

339

340

341

342

343

344

345

346

347

348

349

350

351

352

353

354

355

356

357

358

359

360

361

362

Based on the results presented above, we propose in Figure 4 the main pathways of VL photonitration in aqueous solution under slightly acidic conditions. The first step of the reaction likely involves the abstraction of a hydrogen atom from the OH group on VL by •NO<sub>2</sub>, yielding a phenoxy resonance stabilized radical (A<sub>1</sub>) and a HNO<sub>2</sub>. <sup>56, 64</sup> Unlike the powerful •OH radical, •NO<sub>2</sub> is unable to attach directly to an aromatic carbon atom or abstract a hydrogen atom from the aromatic ring.<sup>56</sup> The H-abstraction step destroys the aromaticity of VL, which allows the addition of a second •NO2 to A1 to form A2 - an intermediate. The rearomatization of A2 yields 5NV (A<sub>4</sub>) through hydrogen rearrangement with the assistance of a water molecule, which probably involves A<sub>3</sub> as a transition state. 64-67 In this step, the water molecule serves as a bridge, accepting the hydrogen atom from the aromatic ring and simultaneously donating another hydrogen to the quinonic oxygen of A<sub>2</sub>.<sup>64</sup> Since this reaction has a much lower energy barrier compared to the reaction without water, <sup>68</sup> the water molecule plays a catalytic role on the formation of nitrated products. Although it is possible that •NO reacts with  $A_1$  to form 5-nitrosovanillin  $(A_5)$ , <sup>56</sup> the kinetic results of this study suggests that •NO is not sufficiently reactive to initiate the formation of the phenoxy radical of VL (A<sub>1</sub>). Nevertheless, once formed, A<sub>5</sub> is prone to undergo further oxidation by •NO<sub>2</sub> to form 5NV (A<sub>4</sub>).<sup>69</sup>

The hydroxyl and methoxy groups on VL are *ortho-para* directors and the aldehyde group is a *meta* director. <sup>70</sup> The directing effects of the three substituents work together to determine that the position *ortho* to OH group is the most reactive for  ${}^{\bullet}NO_2$  or  ${}^{\bullet}NO$ , responsible for 5NV being the most abundant product of VL oxidation. A H-abstraction from the OH group on 5NV (A<sub>4</sub>) by  ${}^{\bullet}NO_2$ , followed by  ${}^{\bullet}NO_2$  addition to the position occupied by the aldehyde group, produces an intermediate (A<sub>6</sub>). The rearomatization of A<sub>6</sub> gives 4,6-dinitroguaiacol (A<sub>7</sub>) through a H<sub>2</sub>O-assisted rearrangement of a hydrogen atom in the aldehyde group to the quinonic

oxygen of A<sub>6</sub> and a CO elimination.<sup>71</sup> Note that H-abstraction from the aldehyde group by •NO<sub>2</sub> is also possible as the C-H bond of the carbonyl is relatively weak.<sup>72</sup>, <sup>73</sup> The H-abstraction from the aldehyde group on 5NV (A<sub>4</sub>) by •NO<sub>2</sub>, followed by O<sub>2</sub> addition, may lead to the formation of a peroxy radical (A<sub>8</sub>), <sup>74</sup> which subsequently reacts via two channels. One is to interact with HO<sub>2</sub>• to form 5-nitrovanillic acid (A<sub>9</sub>) <sup>75</sup> and the other involves being rapidly reduced to an alkoxy radical  $(A_{10})$  by •NO. A<sub>10</sub> undergoes decarboxylation to give the aryl species (A<sub>11</sub>),<sup>74</sup> which can combine with A<sub>1</sub> to form the derivative of VL dimmer (A<sub>12</sub>) or • NO<sub>2</sub> to form 4,6-dinitroguaiacol (A<sub>7</sub>). The •NO<sub>2</sub> addition to the A<sub>1</sub> ring position occupied by the aldehyde group, followed by H-rearrangement catalyzed by a water molecule and CO elimination, generates 4NG (A<sub>13</sub>). The addition of •NO to A<sub>1</sub> ring position occupied by the aldehyde group, followed by H<sub>2</sub>O catalyzation, results in the formation of 4-nitrosoguaiacol ( $A_{14}$ ), which can be further oxidized by  $\cdot NO_2$  to form 4NG ( $A_{13}$ ). H-abstraction from the OH group of 4NG (A<sub>13</sub>) by •NO<sub>2</sub>, followed by •NO<sub>2</sub> addition, produces 4,6-dinitroguaiacol (A<sub>7</sub>). The pathways of  $A_8 \rightarrow A_9$  and  $A_8 \rightarrow A_{11}$  have been reported in gas phase, but our work indicates that these reaction mechanisms are also applicable to atmospheric aqueous phase.

In order to investigate the influence of NO<sub>2</sub>/VL molar ratio on the molecular composition of the reaction products, air-saturated solution containing 100  $\mu$ M NO<sub>2</sub> and 100  $\mu$ M VL was irradiated with simulated sunlight at pH 5.0 for 3 h. The TIC and the corresponding average MS of the reaction products are presented in Figure S7a and Figure S8, respectively. Same as the nitration products detected in the 10:1 (molar ratio) solution of NO<sub>2</sub>/VL, 5NV (RT = 9.72 min), 4NG (RT = 10.12 min), and C<sub>14</sub>H<sub>10</sub>N<sub>2</sub>O<sub>6</sub> (RT = 11.15 min) were identified in the oxidative products of 1:1 solution as well. Furthermore, the chromatogram of the 1:1 NO<sub>2</sub>-/VL solution shows a few additional peaks between RT = 6 min and 7 min (see the inset of Figure S7). The peak at RT = 6.48 min is assigned to 3,4-dihydroxybenzaldehyde (m/z = 137.02428), which is a demethoxylated aromatic product of VL oxidation. The peak at RT = 6.61 min corresponds to a poly-hydroxylated product, 5,6-dihydroxyvanillin (m/z = 183.02980). The peaks at RT = 6.78 and 6.89 min are assigned to 5-hydroxyvanillin (m/z =

167.03487) and its isomer. These results suggest that hydroxylation is an important reaction pathway for VL oxidation at equal molar concentrations of NO<sub>2</sub> and VL. The reason may be that VL can also react with •OH generated by nitrite photolysis (reactions 5 and 6) and hence efficiently competes with NO<sub>2</sub> for •OH at low NO<sub>2</sub>-/VL molar ratio. The proposed pathways for •OH-mediated oxidation of VL are presented in Figure S9. The reaction between •OH and VL is mainly dominated by hydroxylation of the aromatic ring. For example, ipso-addition of •OH to the ring position occupied by the methoxyl group, followed by the elimination of a methanol molecule, results in the formation of a semiguinone radical (B<sub>1</sub>). <sup>76</sup> B<sub>1</sub> then can abstract a H atom from HO<sub>2</sub> • and forms 3,4-dihydroxybenzaldehyde (B<sub>2</sub>).<sup>74</sup> A previous study has indeed shown that the ipso-addition of •OH is a predominant pathway compared to the ortho- and para-addition of • OH to the ring of methoxyphenol in aqueous phase.<sup>77</sup> In addition, the *ortho*-addition of •OH to the ring, followed by H-abstraction by O2, may result in the formation of 5-hydroxyvanillin (B<sub>3</sub>), <sup>78</sup> which can be further oxidized to 5,6-dihydroxyvanillin (B<sub>4</sub>) through a second •OH addition and H-abstraction by O<sub>2</sub>. Our results highlight that the NO<sub>2</sub>/phenol molar ratio has a significant impact on the molecular composition of the photooxidative products from phenol reactions with nitrite in aqueous solution. As far as we know, the influence of NO<sub>2</sub>/phenol molar ratio on the molecular composition of the products has scarcely been investigated before.

413

414

415

416

417

418

419

420

421

422

393

394

395

396

397

398

399

400

401

402

403

404

405

406

407

408

409

410

411

412

#### 3.3 The pH-dependent light absorbance of the nitrophenol products

There is increasing evidence that nitrophenols are important chromophores in atmospheric BrC. <sup>26, 79</sup> This study reveals that nitrophenols (primarily 5NV and 4NG) are the major oxidation products from the photoreactions of nitrite and VL. However, the light absorbance of the nitrophenol products is found to be strongly dependent on the solution pH. As shown in Figure 5, the UV-vis absorption spectra of 5NV and 4NG present significant red-shifts and increases in visible light absorption with increasing pH. This is because the deprotonation of a nitrophenol molecule at higher pH changes its electronic structure, which greatly affects the absorption characteristics

of the chromophore and causes more intense absorption at wavelengths above the 290-370 nm. Figure S10 illustrates the underlying mechanism for such change: when 5NV or 4NG deprotonates, an ortho- or para-nitro group is capable of attracting a portion of the negative charge to its own oxygen atoms through the induced and conjugated effects of the nitro group, resulting in the extension of the chromophore from the electro-donating group (e.g., -O<sup>-</sup>) to the electron-withdrawing group (e.g., -NO<sub>2</sub>) through the aromatic ring. <sup>80, 81</sup> The delocalization of the negative charge in phenolates thus causes a pronounced red-shift in absorbance.<sup>79</sup> As a result, under higher pH conditions (such as pH 9.0), where the phenolate anion of 5NV or 4NG becomes the dominant species, both nitrophenols absorb significantly in the visible light region (Figure 5). In contrast, when 5NV or 4NG exists in the undissociated form, it is energetically unfavorable for the delocalization of an unshared electron in the OH function group into the nitro group through the ring (SI Figure S10) to occur. This is because such electron delocalization would involve the separation of the positive charge and the negative charge that costs energy. 82 For these reasons, at low pH (such as pH 3.0), nearly all 5NV or 4NG molecules are present in undissociated form, their absorption spectra show features characteristic of separate, non-interacting chromophores, with the wavelength of maximum absorbance  $(\lambda_{max})$  locating in the UV region (Figure 5).

423

424

425

426

427

428

429

430

431

432

433

434

435

436

437

438

439

440

441

442

443

444

445

446

447

448

449

450

451

452

The –CHO group on a phenolic molecule behaves in a similar fashion as the – NO<sub>2</sub> group. The deprotonation of VL facilitates the electron delocalization from the electro-donating group –O to the electron-withdrawing group –CHO (Figure S11), thus gives rise to a red-shift in absorbance at higher pH (Figure S12). However, the deprotonated VL does not absorb the visible light absorbance as the deprotonated 4NG does (Figure 5b), which suggests the electron delocalization between the –O group and the –CHO group is weaker than that between the –O group and the –NO<sub>2</sub> group. Generally, when an electron-withdrawing group, such as nitro group or aldehyde group, is situated *para* or *ortho* to OH group of phenol, increasing pH may cause a pronounced increase in absorption at longer wavelengths for the substituted phenolic species. To the best of our knowledge, this study is the first to provide a

mechanistic explanation for the pH-dependent light absorbance of nitrophenols.

454

455

456

457

458

459

460

461

462

463

464

465

466

467

468

469

470

471

472

473

474

475

476

477

478

479

480

481

482

453

### 4. Atmospheric Implications

This study reveals that nitrite-mediated photooxidation of vanillin – a phenolic carbonyl compound emitted in large amounts from biomass burning processes – can be a significant source of nitrophenols (NPs) under conditions representative of atmospheric water. It also demonstrates that the production of NPs is strongly influenced by reaction conditions such as NO<sub>2</sub>-/VL molar ratio, pH of the solution, and the presence of •OH scavengers. In the solution with high nitrite/phenols molar ratio, • NO<sub>2</sub> is found to be the dominant reacting radicals that initiates the photooxidation of VL. In addition, our results reveal that •OH scavengers only have a limited impact on the photonitration of VL by NO<sub>2</sub>, which highlights the important roles that nitrite photochemistry may play in the atmospheric aqueous nitration processes. The molecular composition of the products from phenol reactions with nitrite is influenced by the NO<sub>2</sub>-/VL molar ratio in solution, a high NO<sub>2</sub>-/VL molar ratio (e.g., molar ratio of 10) was shown to strongly favor the formation of nitration products. Considering that NPs are toxic for living organisms and can be a significant threat to human health, our findings may have important implications for understanding the health impacts of particulate matter, especially in urban areas influenced by biomass burning emissions. In many US and European cities, burning of wood is a common method for heating during wintertime. Coupled with foggy meteorological conditions, which are frequent in areas such as the Central Valley of California and the Po Valley of Italy in winter, the active emissions of NO<sub>x</sub> from fossil fuel combustion and phenols from biomass burning may promote the formation of NPs, thus acerbate the toxicity of airborne particles.

Another important finding from this study is that pH is a key determinant of the oxidation rate of VL, photoformation rate of NPs, as well as the light absorption properties of the NP products in aqueous phase. NPs are well-known brown carbon (BrC) species with pronounced absorbance bands within the UV and visible light region. <sup>83, 84</sup> The UV-vis spectra of NPs were found to present significant red-shifts and

absorption increases when the pH in the solution increase. Furthermore, according to a few recent studies, BrC in ambient particles displayed systematic increases in absorption with increasing pH as well. These findings suggest that pH-dependent light absorptivity may be a more universal property of atmospheric BrC. Given the fact that the pH in atmospheric condensed phases varies widely from 0 to 9, the influence of pH on BrC absorption properties needs to be thoroughly studied and properly represented in aerosol models. In this study, a mechanistic explanation is provided for the effects that pH has on the light absorption properties of functionalized phenols including NPs. This information is important for better elucidating the role that BrC plays in influencing the radiative balance of the atmosphere.

494

495 496

483

484

485

486

487

488

489

490

491

492

493

## **Supporting information**

- 497 Materials and reagents, additional experimental details, analytical procedures, Table
- 498 S1 and S2, Figure S1-S12.

499

500

# Acknowledgements

This work was supported by the National Natural Science Foundation of China (Nos. 91544224, 41775150, 41827804). QZ acknowledges the funding from the US National Science Foundation grant number AGS- 1649212.

504

505

# Reference

- 506 (1) Singh, H. B.; Salas, L. J.; Cantrell, B. K.; Redmond, R. M. Distribution of aromatic hydrocarbons
- 507 in the ambient air. Atmos. Environ. 1985, 19 (11), 1911-1919.
- 508 (2) Shrivastava, M.; Cappa, C. D.; Fan, J.; Goldstein, A. H.; Guenther, A. B.; Jimenez, J. L.; Kuang,
- 509 C.; Laskin, A.; Martin, S. T.; Ng, N. L. Recent advances in understanding secondary organic aerosol:
- Implications for global climate forcing. Rev. Geophys. 2017, 55 (2), 509-559.
- 511 (3) Ervens, B.; Turpin, B.; Weber, R. Secondary organic aerosol formation in cloud droplets and
- aqueous particles (aqSOA): a review of laboratory, field and model studies. Atmos. Chem. Phys. 2011,
- 513 *11* (21), 11069-11102.
- 514 (4) Hoffmann, E. H.; Tilgner, A.; Wolke, R.; Böge, O.; Walter, A.; Herrmann, H. Oxidation of
- 515 substituted aromatic hydrocarbons in the tropospheric aqueous phase: kinetic mechanism development
- and modelling. Physical Chemistry Chemical Physics 2018, 20 (16), 10960-10977.
- 517 (5) Herrmann, H.; Schaefer, T.; Tilgner, A.; Styler, S. A.; Weller, C.; Teich, M.; Otto, T. Tropospheric
- 518 aqueous-phase chemistry: kinetics, mechanisms, and its coupling to a changing gas phase. Chem. Rev.

- **2015,** *115* (10), 4259-4334.
- 520 (6) Xu, C.; Wang, L. Atmospheric oxidation mechanism of phenol initiated by OH radical. The
- 521 *Journal of Physical Chemistry A* **2013**, *117* (11), 2358-2364.
- 522 (7) Kitanovski, Z.; Čusak, A.; Grgić, I.; Claeys, M. Chemical characterization of the main products
- formed through aqueous-phase photonitration of guaiacol. *Atmos. Meas. Tech.* **2014,** 7 (8), 2457-2470.
- 524 (8) Smith, J. D.; Kinney, H.; Anastasio, C. Phenolic carbonyls undergo rapid aqueous
- 525 photodegradation to form low-volatility, light-absorbing products. Atmos. Environ. 2016, 126, 36-44.
- 526 (9) Chang, J. L.; Thompson, J. E. Characterization of colored products formed during irradiation of
- 527 aqueous solutions containing H2O2 and phenolic compounds. Atmos. Environ. 2010, 44 (4), 541-551.
- 528 (10) Schauer, J. J.; Kleeman, M. J.; Cass, G. R.; Simoneit, B. R. Measurement of emissions from air
- pollution sources. 3. C1- C29 organic compounds from fireplace combustion of wood. *Environmental*
- 530 science & technology **2001**, *35* (9), 1716-1728.
- 531 (11) Ji, Y.; Zhao, J.; Terazono, H.; Misawa, K.; Levitt, N. P.; Li, Y.; Lin, Y.; Peng, J.; Wang, Y.; Duan, L.
- 532 Reassessing the atmospheric oxidation mechanism of toluene. Proc. Natl. Acad. Sci. U.S.A. 2017,
- 533 201705463.
- 534 (12) Schwantes, R. H.; Schilling, K. A.; McVay, R. C.; Lignell, H.; Coggon, M. M.; Zhang, X.;
- 535 Wennberg, P. O.; Seinfeld, J. H. Formation of highly oxygenated low-volatility products from cresol
- 536 oxidation. Atmos. Chem. Phys. 2017, 17 (5), 3453-3474.
- 537 (13) Yu, L.; Smith, J.; Laskin, A.; Anastasio, C.; Laskin, J.; Zhang, Q. Chemical characterization of
- 538 SOA formed from aqueous-phase reactions of phenols with the triplet excited state of carbonyl and
- 539 hydroxyl radical. Atmos. Chem. Phys. 2014, 14 (24), 13801-13816.
- 540 (14) Smith, J. D.; Sio, V.; Yu, L.; Zhang, Q.; Anastasio, C. Secondary organic aerosol production from
- aqueous reactions of atmospheric phenols with an organic triplet excited state. Environ. Sci. Technol.
- **2014,** 48 (2), 1049-1057.
- 543 (15) Yee, L.; Kautzman, K.; Loza, C.; Schilling, K.; Coggon, M.; Chhabra, P.; Chan, M.; Chan, A.;
- Hersey, S.; Crounse, J. Secondary organic aerosol formation from biomass burning intermediates:
- 545 phenol and methoxyphenols. *Atmos. Chem. Phys.* **2013,** *13* (16), 8019-8043.
- 546 (16) Atkinson, R.; Aschmann, S. M.; Arey, J. Reactions of hydroxyl and nitrogen trioxide radicals with
- 547 phenol, cresols, and 2-nitrophenol at 296.+-. 2 K. Environ. Sci. Technol. 1992, 26 (7), 1397-1403.
- 548 (17) Sandhiya, L.; Kolandaivel, P.; Senthilkumar, K. Mechanism and kinetics of the atmospheric
- oxidative degradation of dimethylphenol isomers initiated by OH radical. J. Phys. Chem. A 2013, 117
- 550 (22), 4611-4626.
- 551 (18) Bolzacchini, E.; Bruschi, M.; Hjorth, J.; Meinardi, S.; Orlandi, M.; Rindone, B.; Rosenbohm, E.
- Gas-phase reaction of phenol with NO3. Environ. Sci. Technol. 2001, 35 (9), 1791-1797.
- 553 (19) Huang, D. D.; Zhang, Q.; Cheung, H. H.; Yu, L.; Zhou, S.; Anastasio, C.; Smith, J. D.; Chan, C. K.
- Formation and Evolution of aqSOA from Aqueous-Phase Reactions of Phenolic Carbonyls:
- 555 Comparison between Ammonium Sulfate and Ammonium Nitrate Solutions. Environ. Sci. Technol.
- **2018**, *52* (16), 9215-9224.
- 557 (20) Vione, D.; Maurino, V.; Minero, C.; Pelizzetti, E. New processes in the environmental chemistry
- of nitrite: nitration of phenol upon nitrite photoinduced oxidation. Environ. Sci. Technol. 2002, 36 (4),
- 559 669-676.
- 560 (21) Vidović, K.; L Jurković, D.; M.; Krof A.; Grgić, I. Nighttime aqueous-phase
- formation of nitrocatechols in the atmospheric condensed phase. Environ. Sci. Technol. 2018, 52 (17),
- 562 9722-9730.

- 563 (22) Harrison, M. A.; Barra, S.; Borghesi, D.; Vione, D.; Arsene, C.; Olariu, R. I. Nitrated phenols in
- the atmosphere: a review. *Atmos. Environ.* **2005,** *39* (2), 231-248.
- 565 (23) Leuenberger, C.; Czuczwa, J.; Tremp, J.; Giger, W. Nitrated phenols in rain: atmospheric
- occurrence of phytotoxic pollutants. *Chemosphere* **1988**, *17* (3), 511-515.
- 567 (24) Grundlingh, J.; Dargan, P. I.; El-Zanfaly, M.; Wood, D. M. 2, 4-dinitrophenol (DNP): a weight
- loss agent with significant acute toxicity and risk of death. J. Med. Toxicol. 2011, 7 (3), 205.
- 569 (25) Laskin, A.; Laskin, J.; Nizkorodov, S. A. Chemistry of atmospheric brown carbon. Chem. Rev.
- **2015,** *115* (10), 4335-4382.
- 571 (26)Desyaterik, Y.; Sun, Y.; Shen, X.; Lee, T.; Wang, X.; Wang, T.; Collett, J. L. Speciation of -brown"
- 572 carbon in cloud water impacted by agricultural biomass burning in eastern China. Journal of
- 573 *Geophysical Research: Atmospheres* **2013**, *118* (13), 7389-7399.
- 574 (27) Kitanovski, Z.; Grgić, I.; Vermeylen, R.; Claeys, M.; Maenhaut, W. Liquid chromatography
- 575 tandem mass spectrometry method for characterization of monoaromatic nitro-compounds in
- atmospheric particulate matter. J. Chromatogr. A 2012, 1268, 35-43.
- 577 (28) Heal, M. R.; Harrison, M. A.; Cape, J. N. Aqueous-phase nitration of phenol by N2O5 and ClNO2.
- 578 Atmos. Environ. **2007**, 41 (17), 3515-3520.
- 579 (29) Krof A.; Grilc, M.; Grgić, I. Unraveling pathways of Guaiacol nitration in atmospheric waters:
- 580 nitrite, a source of reactive nitronium ion in the atmosphere. Environ. Sci. Technol. 2015, 49 (15),
- 581 9150-9158.
- 582 (30) Vione, D.; Maurino, V.; Minero, C.; Pelizzetti, E. Aqueous atmospheric chemistry: Formation of 2,
- 583 4-dinitrophenol upon nitration of 2-nitrophenol and 4-nitrophenol in solution. Environ. Sci. Technol.
- **2005**, *39* (20), 7921-7931.
- 585 (31) Vione, D.; Maurino, V.; Minero, C.; Pelizzetti, E. Nitration and photonitration of naphthalene in
- 586 aqueous systems. Environ. Sci. Technol. 2005, 39 (4), 1101-1110.
- 587 (32) Brown, S. S.; Stutz, J. Nighttime radical observations and chemistry. Chem. Soc. Rev. 2012, 41
- 588 (19), 6405-6447.
- 589 (33) Rossi, M. J. Heterogeneous reactions on salts. *Chem. Rev.* **2003**, *103* (12), 4823-4882.
- 590 (34) Lammel, G.; NeiláCape, J. Nitrous acid and nitrite in the atmosphere. Chem. Soc. Rev. 1996, 25
- 591 (5), 361-369.
- 592 (35) Mack, J.; Bolton, J. R. Photochemistry of nitrite and nitrate in aqueous solution: a review. J.
- 593 *Photochem. Photobiol., A* **1999,** *128* (1-3), 1-13.
- 594 (36) Fischer, M.; Warneck, P. Photodecomposition of nitrite and undissociated nitrous acid in aqueous
- 595 solution. J. Phys. Chem. 1996, 100 (48), 18749-18756.
- 596 (37) Anastasio, C.; Chu, L. Photochemistry of nitrous acid (HONO) and nitrous acidium ion
- 597 (H2ONO+) in aqueous solution and ice. *Environ. Sci. Technol.* **2009**, *43* (4), 1108-1114.
- 598 (38) Vione, D.; Belmondo, S.; Carnino, L. A kinetic study of phenol nitration and nitrosation with
- 599 nitrous acid in the dark. *Environ. Chem. Lett* **2004**, *2* (3), 135-139.
- 600 (39) Bunton, C.; Hughes, E.; Ingold, C.; Jacobs, D.; Jones, M.; Minkoff, G.; Reed, R. 512. Kinetics
- and mechanism of aromatic nitration. Part VI. The nitration of phenols and phenolic ethers: the
- 602 concomitant dealkylation of phenolic ethers. The role of nitrous acid. J. Chem. Soc. 1950, 2628-2656.
- 603 (40) Vione, D.; Maurino, V.; Minero, C.; Borghesi, D.; Lucchiari, M.; Pelizzetti, E. New processes in
- the environmental chemistry of nitrite. 2. The role of hydrogen peroxide. Environ. Sci. Technol. 2003,
- 605 37 (20), 4635-4641.
- 606 (41) Goldstein, S.; Lind, J.; Merényi, G. Chemistry of peroxynitrites as compared to peroxynitrates.

- 607 Chem. Rev. 2005, 105 (6), 2457-2470.
- 608 (42) Vione, D.; Maurino, V.; Minero, C.; Pelizzetti, E. Phenol photonitration upon UV irradiation of
- 609 nitrite in aqueous solution I: Effects of oxygen and 2-propanol. Chemosphere 2001, 45 (6-7), 893-902.
- 610 (43) Kim, D.-h.; Lee, J.; Ryu, J.; Kim, K.; Choi, W. Arsenite oxidation initiated by the UV photolysis
- of nitrite and nitrate. *Environ. Sci. Technol.* **2014**, *48* (7), 4030-4037.
- 612 (44) Rabani, J.; Matheson, M. S. Pulse radiolytic determination of p K for hydroxyl ionic dissociation
- 613 in water. J. Am. Chem. Soc. 1964, 86 (15), 3175-3176.
- 614 (45) Simoneit, B. R. Biomass burning—a review of organic tracers for smoke from incomplete
- 615 combustion. Appl. Geochem. 2002, 17 (3), 129-162.
- 616 (46) Li, Y.; Huang, D.; Cheung, H. Y.; Lee, A.; Chan, C. K. Aqueous-phase photochemical oxidation
- and direct photolysis of vanillin–a model compound of methoxy phenols from biomass burning. Atmos.
- 618 Chem. Phys. 2014, 14 (6), 2871-2885.
- 619 (47) Yaws, C. L., Handbook of vapor pressure: volume 3: Organic compounds C8 to C28. Gulf
- 620 Professional Publishing: 1994; Vol. 3.
- 621 (48) George, K. M.; Ruthenburg, T. C.; Smith, J.; Yu, L.; Zhang, Q.; Anastasio, C.; Dillner, A. M.
- FT-IR quantification of the carbonyl functional group in aqueous-phase secondary organic aerosol from
- 623 phenols. Atmos. Environ. 2015, 100, 230-237.
- 624 (49) Turnock, S.; Mann, G.; Woodhouse, M.; Dalvi, M.; O'Connor, F.; Carslaw, K.; Spracklen, D. The
- 625 Impact of Changes in Cloud Water pH on Aerosol Radiative Forcing. Geophys. Res. Lett. 2019, 46 (7),
- 626 4039-4048.
- 627 (50) Parworth, C. L.; Young, D. E.; Kim, H.; Zhang, X.; Cappa, C. D.; Collier, S.; Zhang, Q.
- Wintertime water soluble aerosol composition and particle water content in Fresno, California. J.
- 629 Geophys. Res.: Atmos. 2017, 122 (5), 3155-3170.
- 630 (51) Yazan, Z.; Erden, S.; Dinç, E. A comparative application of two-way and three-way analysis to
- 631 three-dimensional voltammetric dataset for the pKa determination of vanillin. J. Electroanal. Chem.
- **2018**, *826*, 133-141.
- 633 (52) Arakaki, T.; Miyake, T.; Hirakawa, T.; Sakugawa, H. pH dependent photoformation of hydroxyl
- radical and absorbance of aqueous-phase N (III)(HNO2 and NO2-). Environ. Sci. Technol. 1999, 33
- 635 (15), 2561-2565.
- 636 (53) Lewis, R. S.; Deen, W. M. Kinetics of the reaction of nitric oxide with oxygen in aqueous
- 637 solutions. Chem. Res. Toxicol. 1994, 7 (4), 568-574.
- 638 (54) Goldstein, S.; Czapski, G. Kinetics of nitric oxide autoxidation in aqueous solution in the absence
- and presence of various reductants. The nature of the oxidizing intermediates. J. Am. Chem. Soc. 1995,
- 640 117 (49), 12078-12084.
- 641 (55) Pires, M.; Rossi, M. J.; Ross, D. S. Kinetic and mechanistic aspects of the NO oxidation by O2 in
- aqueous phase. Int. J. Chem. Kinet. 1994, 26 (12), 1207-1227.
- 643 (56) Krof A.; Hu, M.; Grilc, M.; Grgić, I. Underappreciated and complex role of nitrous acid in
- aromatic nitration under mild environmental conditions: the case of activated methoxyphenols. *Environ*.
- 645 Sci. Technol. 2018, 52 (23), 13756-13765.
- 646 (57) Gligorovski, S.; Strekowski, R.; Barbati, S.; Vione, D. Environmental implications of hydroxyl
- 647 radicals (• OH). Chem. Rev. 2015, 115 (24), 13051-13092.
- 648 (58) Zuo, Y.; Hoigne, J. Formation of hydrogen peroxide and depletion of oxalic acid in atmospheric
- water by photolysis of iron (III)-oxalato complexes. Environ. Sci. Technol. 1992, 26 (5), 1014-1022.
- 650 (59) Pryor, W. A.; Squadrito, G. L. The chemistry of peroxynitrite: a product from the reaction of nitric

- oxide with superoxide. Am. J. Physiol-lung. C. 1995, 268 (5), L699-L722.
- 652 (60) Anastasio, C.; Faust, B. C.; Rao, C. J. Aromatic carbonyl compounds as aqueous-phase
- photochemical sources of hydrogen peroxide in acidic sulfate aerosols, fogs, and clouds. 1.
- Non-phenolic methoxybenzaldehydes and methoxyacetophenones with reductants (phenols). Environ.
- 655 Sci. Technol. 1996, 31 (1), 218-232.
- 656 (61) Arakaki, T.; Anastasio, C.; Kuroki, Y.; Nakajima, H.; Okada, K.; Kotani, Y.; Handa, D.; Azechi, S.;
- 657 Kimura, T.; Tsuhako, A. A general scavenging rate constant for reaction of hydroxyl radical with
- organic carbon in atmospheric waters. Environ. Sci. Technol. 2013, 47 (15), 8196-8203.
- 659 (62) Herrmann, H.; Hoffmann, D.; Schaefer, T.; Bräuer, P.; Tilgner, A. Tropospheric aqueous phase
- 660 free radical chemistry: Radical sources, spectra, reaction kinetics and prediction tools.
- 661 *Chemphyschem* **2010,** *11* (18), 3796-3822.
- 662 (63) Warneck, P.; Wurzinger, C. Product quantum yields for the 305-nm photodecomposition of nitrate
- 663 in aqueous solution. J. Phys. Chem. 1988, 92 (22), 6278-6283.
- 664 (64) Bedini, A.; Maurino, V.; Minero, C.; Vione, D. Theoretical and experimental evidence of the
- photonitration pathway of phenol and 4-chlorophenol: a mechanistic study of environmental
- 666 significance. *Photochem. Photobiol. Sci.* **2012**, *11* (2), 418-424.
- 667 (65) Gunaydin, H.; Houk, K. Mechanisms of peroxynitrite-mediated nitration of tyrosine. Chem. Res.
- 668 Toxicol. 2009, 22 (5), 894-898.
- 669 (66) Louw, R.; Santoro, D. Comment on Formation of Nitroaromatic Compounds in Advanced
- Oxidation Processes: Photolysis versus Photocatalysis". Environ. Sci. Technol. 1999, 33 (18),
- 671 3281-3281.
- 672 (67) Ji, Y.; Wang, L.; Jiang, M.; Lu, J.; Ferronato, C.; Chovelon, J.-M. The role of nitrite in sulfate
- 673 radical-based degradation of phenolic compounds: An unexpected nitration process relevant to
- groundwater remediation by in-situ chemical oxidation (ISCO). Water Res. 2017, 123, 249-257.
- 675 (68) Zhang, Q.; Gao, R.; Xu, F.; Zhou, Q.; Jiang, G.; Wang, T.; Chen, J.; Hu, J.; Jiang, W.; Wang, W.
- 676 Role of water molecule in the gas-phase formation process of nitrated polycyclic aromatic
- hydrocarbons in the atmosphere: a computational study. Environ. Sci. Technol. 2014, 48 (9),
- 678 5051-5057.
- 679 (69) Gowenlock, B.; Young, V. Kinetics of the oxidation of aromatic C-nitroso compounds by nitrogen
- 680 dioxide. J. Chem. Soc., Perkin Trans. 2 1997, (9), 1793-1798.
- 681 (70) Jonathan Clayden, N. G., Stuart Warren, Organic Chemistry. . 2nd Edition ed.; OXFORD
- 682 UNIVERSITY PRESS: 2012.
- 683 (71) Asatryan, R.; da Silva, G.; Bozzelli, J. W. Quantum chemical study of the acrolein
- 684 (CH2CHCHO)+ OH+ O2 reactions. J. Phys. Chem. A 2010, 114 (32), 8302-8311.
- 685 (72) Cerón-Carrasco, J.; Bastida, A.; Requena, A.; Zúñiga, J.; Miguel, B. A theoretical study of the
- reaction of β-carotene with the nitrogen dioxide radical in solution. J. Phys. Chem. B 2010, 114 (12),
- 687 4366-4372.
- 688 (73) Giamalva, D. H.; Kenion, G. B.; Church, D. F.; Pryor, W. A. Rates and mechanisms of reactions
- of nitrogen dioxide with alkenes in solution. *J. Am. Chem. Soc.* **1987**, *109* (23), 7059-7063.
- 690 (74) Atkinson, R.; Lloyd, A. C. Evaluation of kinetic and mechanistic data for modeling of
- 691 photochemical smog. J. Phys. Chem. Ref. Data 1984, 13 (2), 315-444.
- 692 (75) Orlando, J. J.; Tyndall, G. S. Laboratory studies of organic peroxy radical chemistry: an overview
- 693 with emphasis on recent issues of atmospheric significance. Chem. Soc. Rev. 2012, 41 (19), 6294-6317.
- 694 (76) Steenken, S.; O'Neill, P. Oxidative demethoxylation of methoxylated phenols and hydroxybenzoic

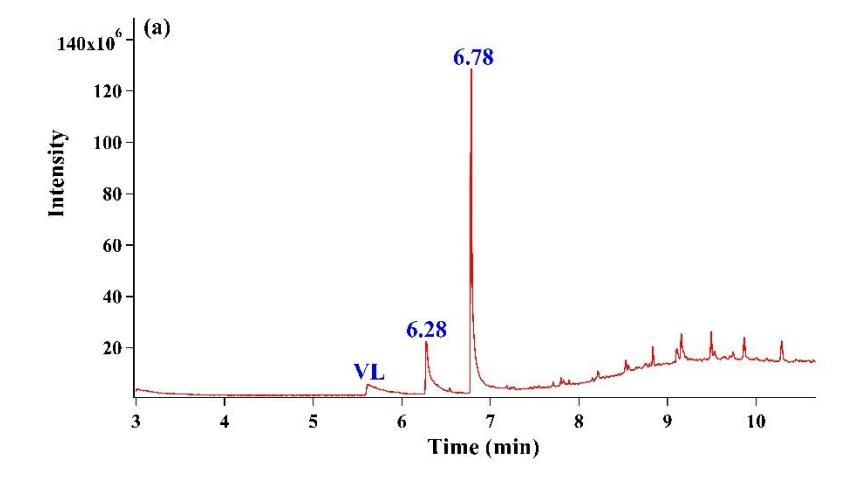
- acids by the hydroxyl radical. An in situ electron spin resonance, conductometric pulse radiolysis and
- 696 product analysis study. J. Phys. Chem. 1977, 81 (6), 505-508.
- 697 (77) Aihara, K.; Urano, Y.; Higuchi, T.; Hirobe, M. Mechanistic studies of selective catechol formation
- from o-methoxyphenols using a copper (II)-ascorbic acid-dioxygen system. J. Chem. Soc., Perkin
- 699 Trans. 2 **1993**, (11), 2165-2170.
- 700 (78) Pang, H.; Zhang, Q.; Wang, H.; Cai, D.; Ma, Y.; Li, L.; Li, K.; Lu, X.; Chen, H.; Yang, X.
- 701 Photochemical Aging of Guaiacol by Fe (III)-Oxalate Complexes in Atmospheric Aqueous Phase.
- 702 Environ. Sci. Technol. 2019, 53 (1), 127-136.
- 703 (79) Mohr, C.; Lopez-Hilfiker, F. D.; Zotter, P.; v t, A. S.; Xu, L.; Ng, N. L.; Herndon, S. C.;
- Williams, L. R.; Franklin, J. P.; Zahniser, M. S. Contribution of nitrated phenols to wood burning
- brown carbon light absorption in Detling, United Kingdom during winter time. Environ. Sci. Technol.
- **2013**, *47* (12), 6316-6324.
- 707 (80) Carey, F. A., Organic Chemistry 4ed.; The McGraw-Hill Companies, Inc.: 2000.
- 708 (81) Williams, D. H.; Fleming, I., Spectroscopic methods in organic chemistry. 6 ed.; McGraw-Hill
- 709 Companies, Inc: 2008.

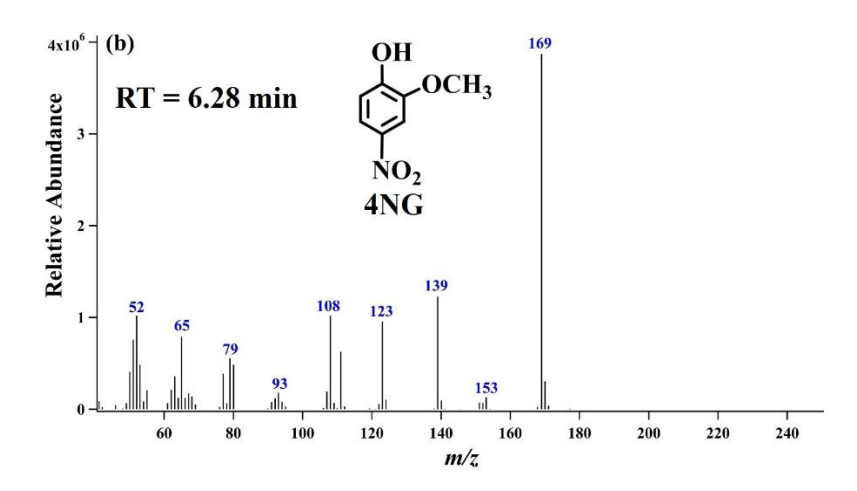
- 710 (82) Solomons, T. G.; Fryhle, C., Organic chemistry. In 10 ed.; John Wiley & Sons, Inc., USA: 2011.
- 711 (83) Zhang, X.; Lin, Y.-H.; Surratt, J. D.; Weber, R. J. Sources, composition and absorption Ångstrom
- 712 exponent of light-absorbing organic components in aerosol extracts from the Los Angeles Basin.
- 713 Environ. Sci. Technol. **2013**, 47 (8), 3685-3693.
- 714 (84) Phillips, S. M.; Bellcross, A. D.; Smith, G. D. Light absorption by brown carbon in the
- 715 southeastern United States is pH-dependent. Environ. Sci. Technol. 2017, 51 (12), 6782-6790.
- 716 (85) Ackendorf, J. M.; Ippolito, M. G.; Galloway, M. M. pH dependence of the
- 717 Imidazole-2-carboxaldehyde hydration equilibrium: implications for atmospheric light absorbance.
- 718 Environ. Sci. Technol. Lett. 2017, 4 (12), 551-555.

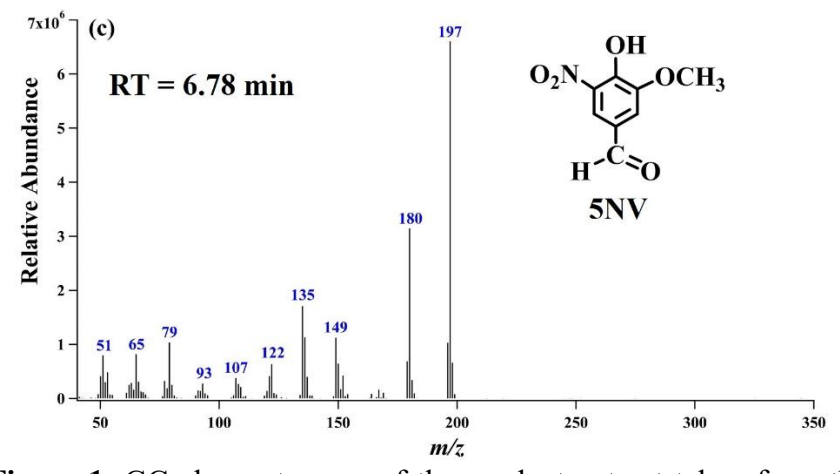
Table 1. Reactions and their rate constants or quantum yield involved in the formation of reactive nitrogen species and hydroxyl radical in the presence of  $NO_2^-/HNO_2$  in aqueous phase under dark and irradiation conditions.

No.	Reaction	$k$ or $\Phi$	Ref.
1	$HNO_2 + H^+ \rightarrow NO^+ + H_2O$		39
2	$2HNO_2 \rightarrow \bullet NO + \bullet NO_2 + H_2O$	$k = 28.6 \text{ M}^{-1} \text{ s}^{-1}$	38
3	$HNO_2 + H_2O_2 \rightarrow HOONO + H_2O$		31
4	$HOONO \rightarrow \bullet NO_2 + \bullet OH$	$k = 0.35 \pm 0.03 \mathrm{s}^{-1}$	41
5	$NO_2^- + hv \rightarrow \bullet NO + \bullet O^-$	$\Phi_{OH,300} = 6.7(\pm 0.9)\%$	35, 36
6	$\bullet O^- + H^+ \leftrightarrow \bullet OH$		35
7	$NO_2^- + \bullet OH \rightarrow \bullet NO_2 + OH^-$	$k = 1.0 \times 10^{10} \mathrm{M}^{-1} \mathrm{s}^{-1}$	35
8	$HNO_2 + hv \rightarrow \bullet NO + \bullet OH$	$\Phi_{OH,300} = 36.2(\pm 4.7)\%$	36, 43
9	$HNO_2 + \bullet OH \rightarrow \bullet NO_2 + H_2O$	$k = 2.6 \times 10^9 \mathrm{M}^{-1} \mathrm{s}^{-1}$	43
10	$\bullet$ NO + O <sub>2</sub> $\leftrightarrow$ ONOO $\bullet$		54
11	$ONOO \bullet + \bullet NO \rightarrow ONOONO$		54
12	$ONOONO \rightarrow 2 \cdot NO_2$		54
13	$NO_2^- + hv \rightarrow NO_2 + e_{aq}^-$	$\Phi < 10^{-3}$	57
14	$O_2 + e_{aq}^- \rightarrow O_2^{\bullet-}$		57
15	$O_2^{\bullet -} + NO_2^- + 2H^+ \rightarrow \bullet NO_2 + H_2O_2$		42
16	$O_2^{\bullet-} + \bullet NO \rightarrow ONOO^-$	$k = (5 \pm 1) \times 10^9 \mathrm{M}^{-1} \mathrm{s}^{-1}$	41
17	$ONOO^- + H^+ \leftrightarrow HOONO$		41
18	$(CH_3)_2CHOH + \bullet OH \rightarrow (CH_3)_2COH \bullet + H_2O$		63
19	$(CH_3)_2COH^{\bullet} + O_2 \rightarrow (CH_3)_2CO + HO_2^{\bullet}$		63
20	•NO + $HO_2$ • $\rightarrow$ HOONO	$k = (3.2 \pm 0.3) \times 10^9 \mathrm{M}^{-1} \mathrm{s}^{-1}$	41

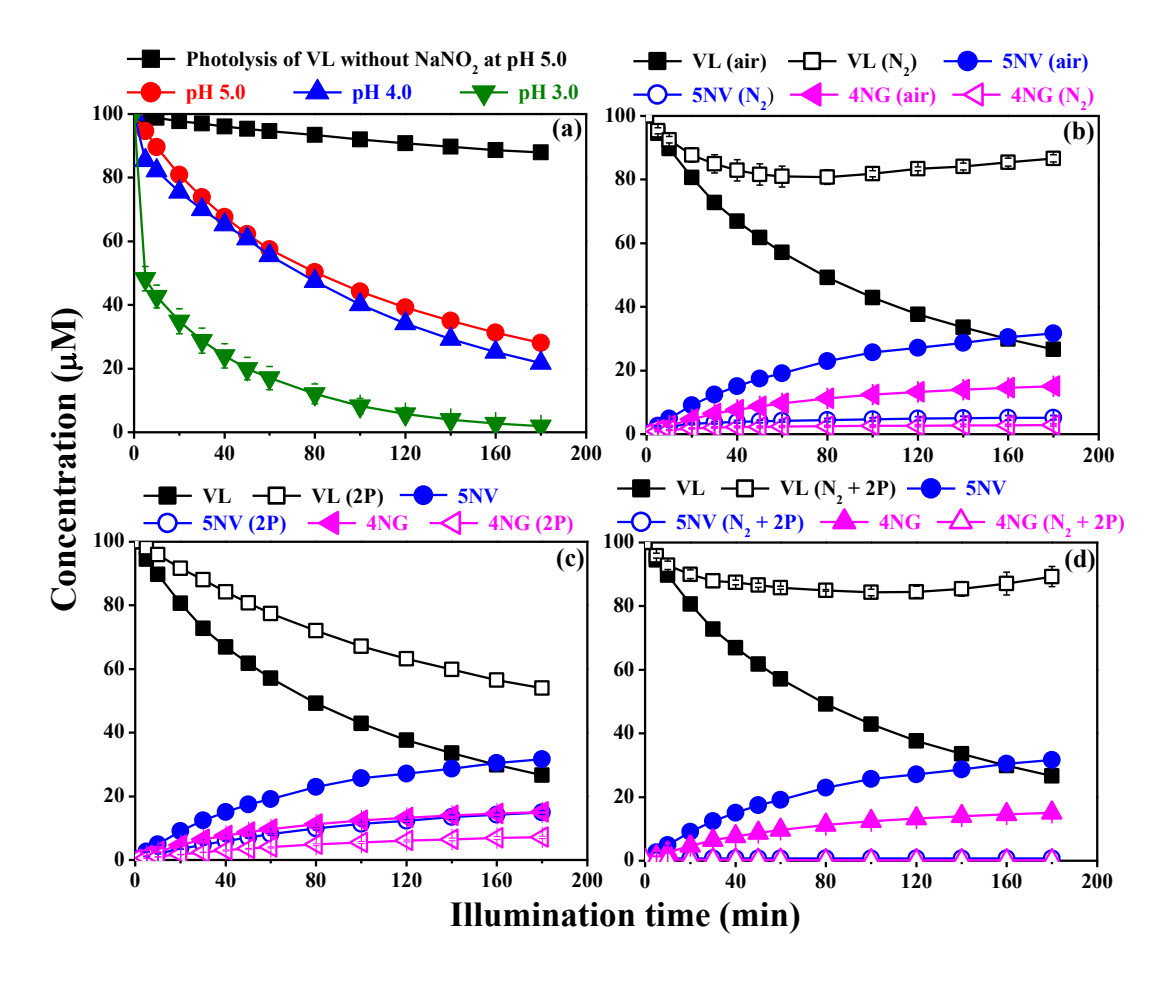




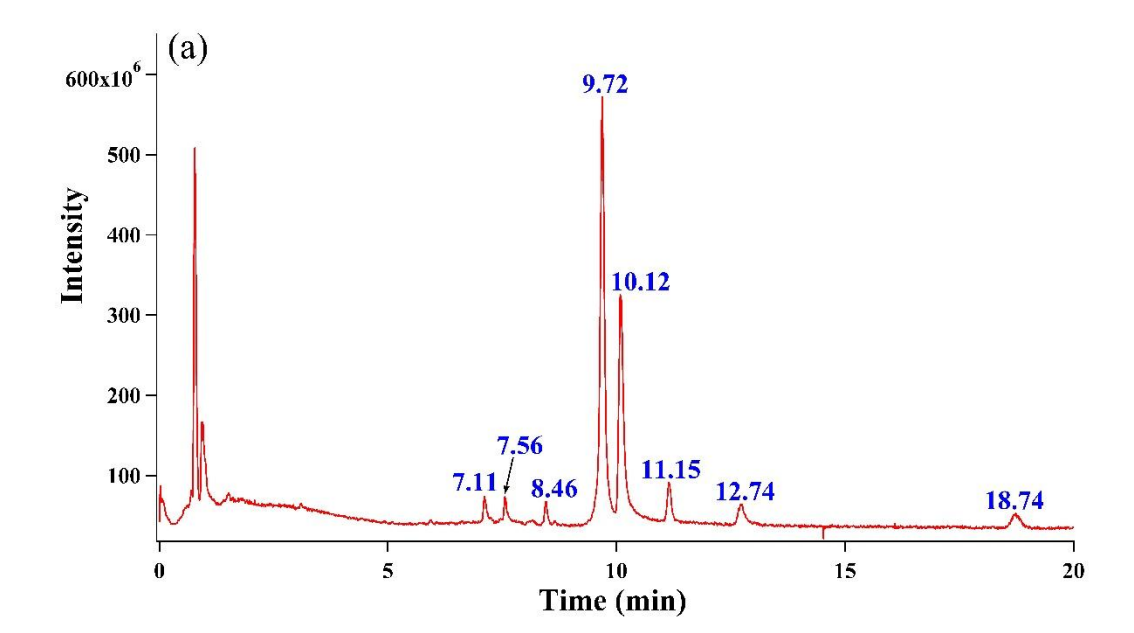




**Figure 1.** GC chromatogram of the product extract taken from the photoreaction of vanillin (VL) with NaNO<sub>2</sub> at 180 min. (a). The corresponding MS patterns for the chromatographic peaks at 6.28 min (b) and 6.78 min (c). The compound for selected chromatographic peak was identified based on NIST library matches. [VL]<sub>0</sub> = 100  $\mu$ M, [NaNO<sub>2</sub>]<sub>0</sub> = 1 mM, pH = 5.0 ± 0.1, air bubbling.



**Figure 2.** (a) Effect of solution pH on the nitrite-mediated photooxidation of VL.  $[VL]_0$ =100 μM,  $[NaNO_2]_0$ =1mM, air saturated solution. (b) Effect of dissolved  $O_2$  on the photooxidation of VL and the formation of 5NV and 4NG.  $[VL]_0$ =100 μM,  $[NaNO_2]_0$ =1mM, pH=5.0±0.1, air bubbling, nitrogen bubbling. (c) Effect of 2-propanol (2P) (500 mM) on the photooxidation of VL and the formation of 5NV and 4NG.  $[VL]_0$ =100 μM,  $[NaNO_2]_0$ =1 mM, pH=5.0±0.1, air bubbling. (d) Effect of 2-propanol (500 mM) on the photooxidation of VL and the formation of 5NV and 4NG under  $N_2$  bubbling conditions.  $[VL]_0$ =100 μM,  $[NaNO_2]_0$ =1 mM, pH=5.0±0.1.



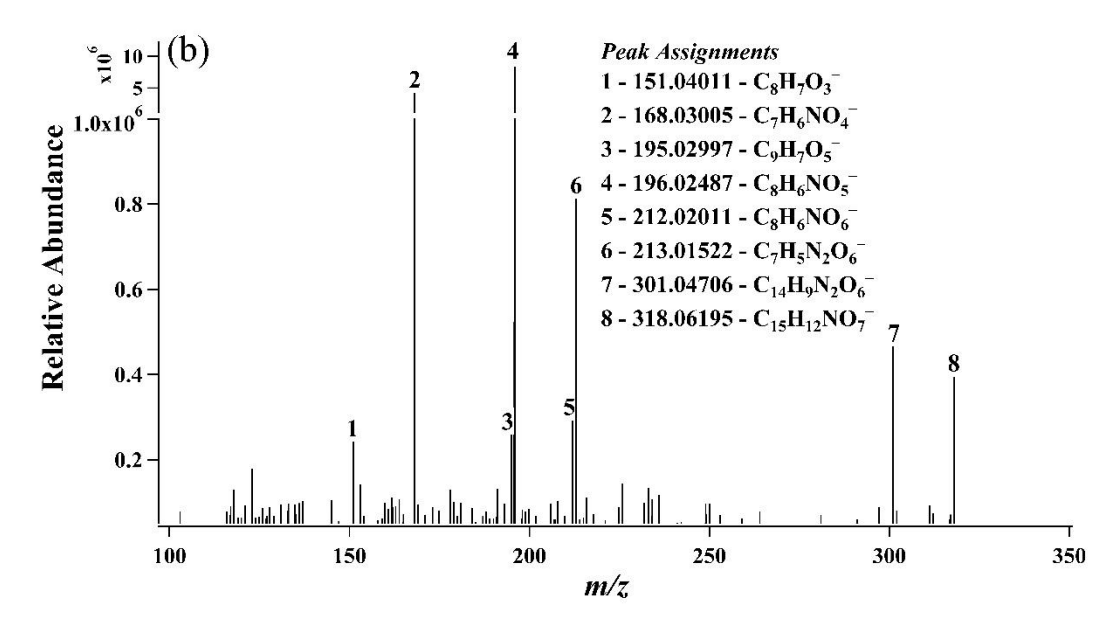


**Figure 3.** (a) The total ion current (TIC) chromatogram and (b) the average (-) ESI mass spectrum for molecules eluted at retention time 5-20 min for the sample taken from the photoreaction of VL with NaNO<sub>2</sub> after 180 min illumination. [VL]<sub>0</sub> = 100  $\mu$ M, [NaNO<sub>2</sub>]<sub>0</sub> = 1 mM,  $\mu$ H = 5.0 ± 0.1, air bubbling.

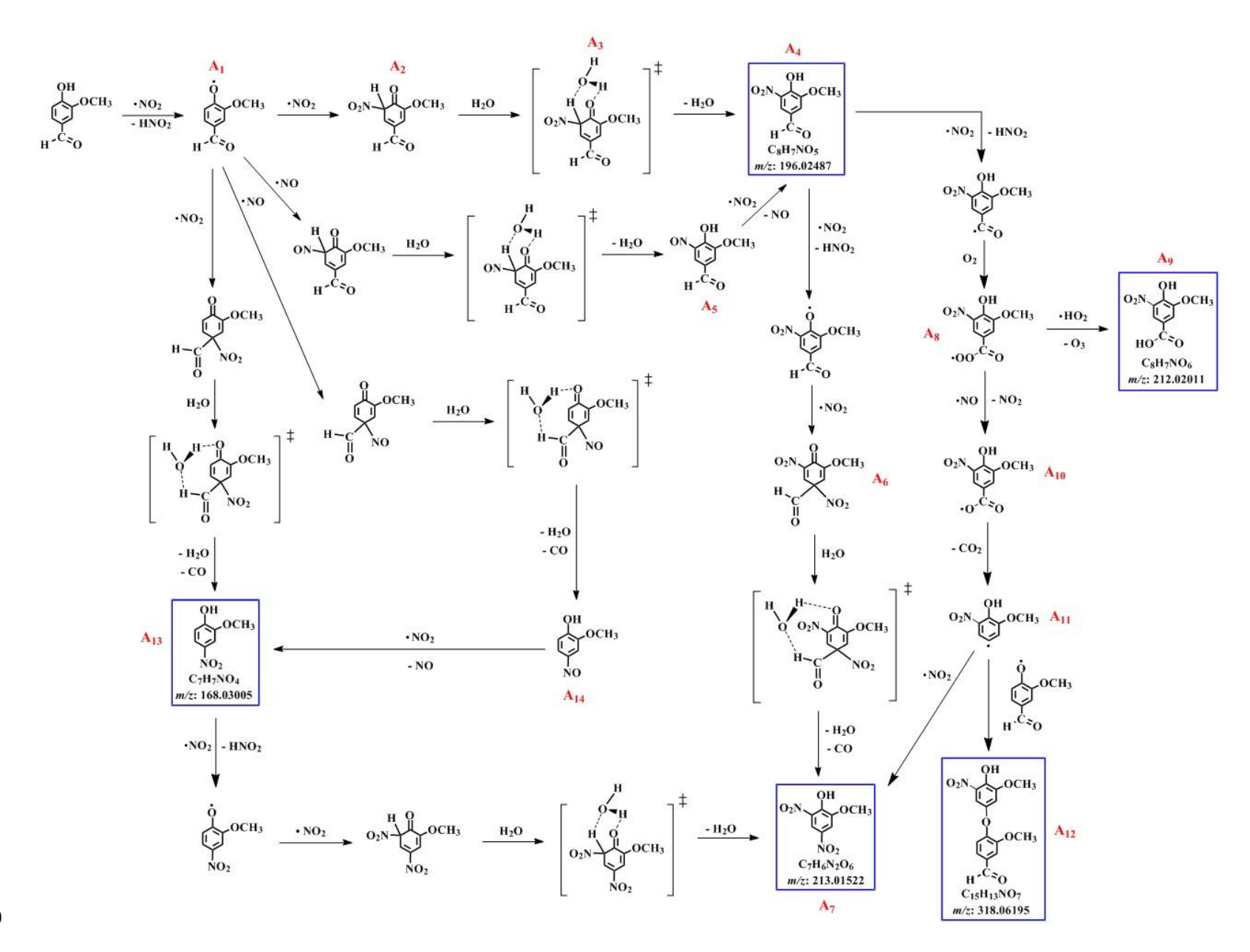


Figure 4. Proposed mechanisms for the formation of nitrated products from the photoreactions of VL with NaNO<sub>2</sub> after 180 min. [VL]<sub>0</sub> = 100  $\mu$ M, [NaNO<sub>2</sub>]<sub>0</sub> = 1 mM, pH = 5.0 ± 0.1, air bubbling.

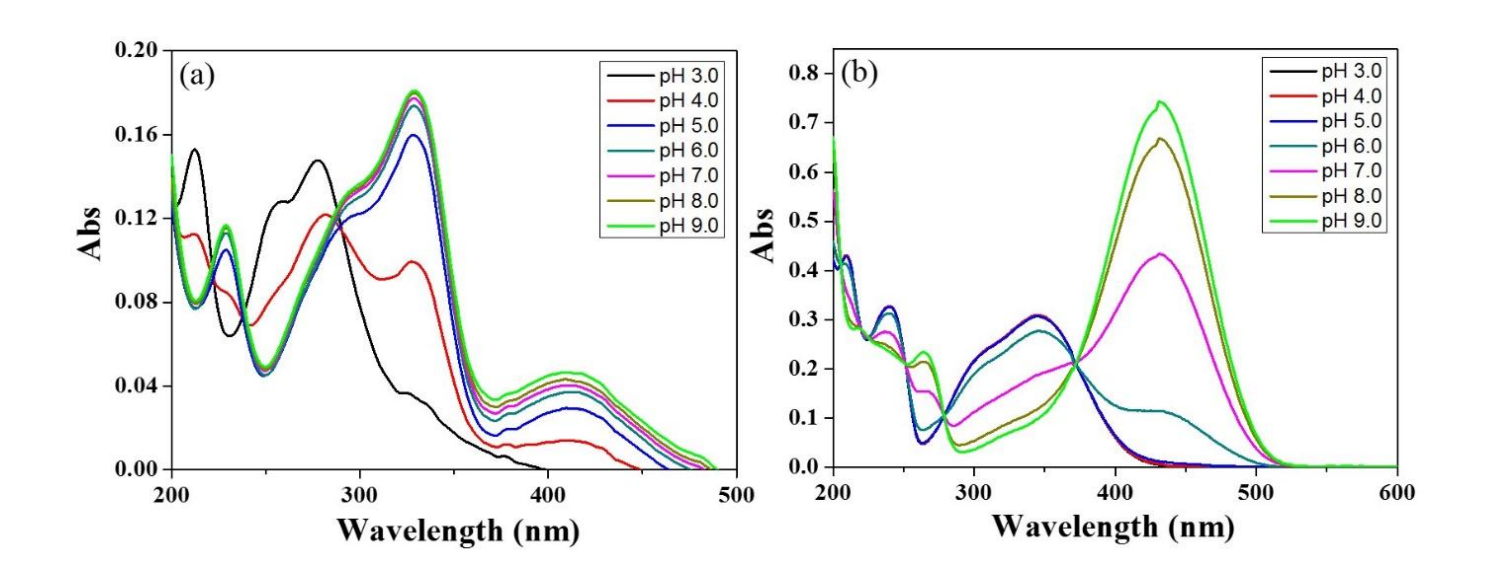
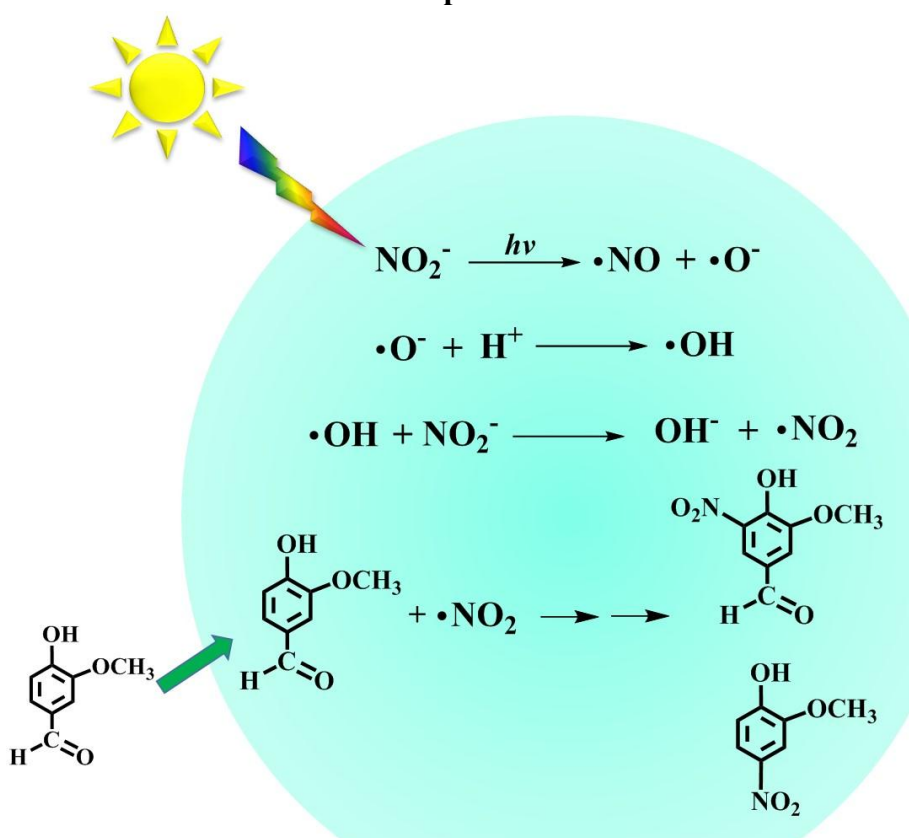


Figure 5. The UV-vis absorption spectra as a function of pH for 10  $\mu$ M 5NV (a) and 30  $\mu$ M 4NG (b).

# **Table of Contents/ Abstract Graphics**



# **Supporting information** Nitrite-Mediated Photooxidation of Vanillin in Atmospheric Aqueous Phase Hongwei Pang<sup>1</sup>, Qi Zhang<sup>2</sup>, Xiaohui Lu<sup>1</sup>, Kangning Li<sup>1</sup>, Hong Chen<sup>1</sup>, Jianmin Chen<sup>1</sup>, Xin Yang<sup>1,3</sup>\*, Yingge Ma<sup>4</sup>, Jialiang Ma<sup>4</sup>, Cheng Huang<sup>4</sup> <sup>1</sup>Shanghai Key Laboratory of Atmospheric Particle Pollution and Prevention, Department of Environmental Science and Engineering, Fudan University, Shanghai 200433, China <sup>2</sup>Department of Environmental Toxicology, University of California, Davis, California 95616, United States <sup>3</sup>Shanghai Institute of Pollution Control and Ecological Security, Shanghai 200092, China <sup>4</sup>State Environmental Protection Key Laboratory of Formation and Prevention of the Urban Air Pollution Complex, Shanghai Academy of Environmental Sciences, Shanghai 200233, China Correspondence to: yangxin@fudan.edu.cn

44	Contents:						
45	Text S1. Materials and reagents—	Page S3					
46	Text S2. Additional experimental details	Page S3					
47	Table S1. An overview of the experiments performed and the analytical devices used						
48	for each experiments	Page S4					
49	Text S3. Analytical procedures—	Page S5					
50							
51	Figure S1. Mole-fraction distribution of the N(III) species at different	pH values					
52		Page S7					
53	Kinetic calculation for the fraction of •OH that reacts with NO <sub>2</sub> and 2	2-propanol					
54		Page S8					
55	Figure S2. Effect of solution pH on the photooxidation kinetics of VL in the	presence					
56	o <del>f nitrite</del>	Page S9					
57	Figure S3. Effect of solution pH on the N(III)-mediated formation of 5NV a	and 4NG					
58		Page S10					
59	Figure S4. The yields of 5NV and 4NG from the photoreaction of VL with	$NO_2$					
60	under different experimental co <del>nditions</del>	Page S11					
61	Figure S5. Effect of solution pH on the N(III)-mediated dark oxidation of V	L					
62		Page S12					
63	Figure S6. Effect of 2-propanol on the photooxidation kinetics of V±	Page S13					
64	Table S2. The products formed through the aqueous-phase photoreactions of	f VL with					
65	NaNO <sub>2</sub> identified with (–) ESI <del>-HRMS</del> —	Page S14					
66	Figure S7. Total ion current (TIC) chromatogram for the oxidative products	at					
67	different NO <sub>2</sub> <sup>-</sup> /VL mo <del>lar ratio</del>	Page S15					
68	Figure S8. Mass spectrum for the oxidative products at NO <sub>2</sub> -/VL molar rati	o of 1:1					
<del>69</del>		Page S16					
70	Figure S9. Proposed mechanisms for the formation of hydroxylated produc	ts					
<del>-71</del>		Page S17					
72	Figure S10. The resonance structures for 5NV and 4NG at high and low sol	ution pH					
<del>73</del>		Page S18					
74	Figure S11. The resonance structures for VL at high and low solution pH-	Page S19					
75	Figure S12. The UV-vis absorption spectra as a function of pH for VL—	Page S20					
76							
77							
78							
79							
80							
81							
82							
83							
84							
85							
86							
87							

# Text S1. Materials and reagents

All chemicals were analytical grade and were used as received. The water employed was deionized and purified by a Millipore purification system (Barnstead NANO Pure, USA). Chemical agents of vanillin (C<sub>8</sub>H<sub>8</sub>O<sub>3</sub>), 5-nitrovanillin (C<sub>8</sub>H<sub>7</sub>NO<sub>5</sub>), 4-nitroguaiacol (C<sub>7</sub>H<sub>7</sub>NO<sub>4</sub>), sodium nitrite (NaNO<sub>2</sub>), 2-propanol (C<sub>3</sub>H<sub>8</sub>O), dichloromethane (CH<sub>2</sub>Cl<sub>2</sub>), sodium chloride (NaCl), sulfuric acid (H<sub>2</sub>SO<sub>4</sub>) and sodium hydroxide (NaOH) were purchased from Sinopharm Chemical Reagent Co. Ltd. (Shanghai, China). Glassware and quartzware were cleaned with a 10% HCl solution, followed by rinsing with deionized water. All solutions were prepared using deionized water.

# Text S2. Additional experimental details

The photochemical reactions were carried out under the following experimental conditions: initial concentrations of vanillin ([vanillin]<sub>0</sub>) was 0.1 mM, initial concentrations of sodium nitrite ([NaNO<sub>2</sub>]<sub>0</sub>) were 1 mM or 0.1mM, and the pH of the solution was adjusted to 3.0, 4.0 or 5.0 using either diluted H<sub>2</sub>SO<sub>4</sub> or NaOH solution. The 10:1 molar ratio of NO<sub>2</sub><sup>-/</sup> vanillin (i.e., 1 mM NaNO<sub>2</sub> and 0.1 mM vanillin) used may reflect the concentration ratio of NO<sub>2</sub> and vanillin found in atmospheric waters in highly polluted urban locations where the concentration of NO<sub>x</sub> is high, while the 1:1 molar ratio of NO<sub>2</sub><sup>-</sup>/ vanillin (i.e., 0.1 mM NaNO<sub>2</sub> and 0.1 mM vanillin) used may reflect the concentration ratio of NO<sub>2</sub> and vanillin found in atmospheric waters in less polluted rural locations where the concentration of NO<sub>x</sub> is relatively low. No buffers were used to adjust the pH value in our experiments as pH variations were \leq 0.4 for all the experiments. In some experiments, 2-propanol was added into the reaction solution in excess (500 mM) to scavenge the photo-formed •OH. The solutions were saturated with high-purity air at the beginning of the experiments or for deaeration experiments, the solution was continuously bubbled with high-purity N<sub>2</sub> starting from 15 min before the reaction until the end of the photoreaction. The dark control experiments were performed in a flask covered with aluminum foil containing 1mM NO<sub>2</sub> and 0.1 mM VL with pH adjusted to 3 to 5 under air-saturated condition. An overview of the experimental conditions performed and the analytical devices used for each experiments was given in table S1. Aliquots of the sample (1mL) were withdrawn at given time intervals and were analyzed by HPLC.

Table S1. An overview of the experiments performed and the analytical devices used for each experiments. Each experiment was repeated three times.

	рН	NO <sub>2</sub>	Vanillin	2-propanol	Air or	Analytical
		concentration	concentration	concentration	$N_2$	devices
					bubbling	
	3	1 mM	0.1 mM		air	HPLC
	4	1 mM	0.1 mM		air	HPLC
						HPLC,
		1 mM	0.1 mM		air	GC-MS,
Simulated						UPLC-HRMS
sunlight		0.1 mM	0.1 mM		air	UPLC-HRMS
	5	1 mM	0.1 mM		N <sub>2</sub>	HPLC
		1 mM	0.1 mM	500 mM	air	HPLC
		1 mM	0.1 mM	500 mM	N <sub>2</sub>	HPLC
			0.1 mM		air	HPLC
	3	1 mM	0.1 mM		air	HPLC
Dark	4	1 mM	0.1 mM		air	HPLC
	5	1 mM	0.1 mM		air	HPLC

### **Text S3. Analytical Procedures**

# S3.1 HPLC analysis

The concentration of the precursors (i.e., vanillin, 5-nitrovanillin and 4-nitroguaiacol) was determined using a HPLC (Agilent 1260) with a Phenomenex Gemini C18 column ( $250 \times 4.60$  mm, 5 µm), photodiode array detector (DAD)] at a flow rate of 1 ml/min. The detection wavelength was 279 nm for vanillin, 277 nm for 5-nitrovanillin, and 345 nm for 4-nitroguaiacol. The mobile phase consisted of 48.5/51.5 (v/v) methanol/water acidified with trifluoroacetic acid (TFA, 0.05%). The injection volume was 50 µl and the retention time of vanillin, 5-nitrovanillin and 4-nitroguaiacol was 5.65 min, 7.64 min and 9.78 min, respectively.

## S3.2 HRMS coupled with UPLC analysis

The analysis of reaction products was carried out using a Q Exactive mass spectrometer (Orbitrap, Thermo Fisher Scientific, mass resolution = 140000 FWHM) equipped with a UltiMate 3000 UHPLC. The samples were separated on a Waters ACQUITY UPLC HSS T3 Column (2.1 × 100 mm, 1.8  $\mu$ m) equipped with a guard column (2.1×5 mm) of the same packing material. The mobile phase consisted of A: 0.1% formic acid in H<sub>2</sub>O and B: 0.1% formic acid in CH<sub>3</sub>CN, with an isocratic elution performed with 71/29 (v/v) mixture of A/B. The flow rate was 0.3 ml/min and injection volume was 5  $\mu$ l. The mass spectra (m/z 90-500) were obtained in negative ion mode after electrospray ionization (ESI). Data acquisition and analysis were conducted by using the Thermo Xcalibur Roadmap software (version 2.2). The mass accuracy limit was set as  $\pm$  5 ppm.

#### S3.3 GC-MS analysis

For gas chromatography/mass spectrometry (GC-MS) analyses, the samples were extracted with  $CH_2Cl_2$  after the addition of salting-out agent NaCl. Then the extracts were concentrated under a gentle stream of high-purity  $N_2$ . The concentrated extract was directly injected into a Thermo FOCUS DSQ GC-MS, equipped with a HP-INNOWax fused-silica capillary column (30 m  $\times$  0.25 mm ID, 0.25  $\mu$ m). The conditions utilized for GC-MS analysis were: carrier gas flow 1 mL/min (He), injector temperature 250 °C, the column temperature was initially held at for 60 °C for 3min, then raised to 300 °C at a rate of 30 °C min-1, with a final holding time of 2 min. The mass spectra were scanned from m/z 29-400 with electron impact ionization technology (EI). Data acquisition and analysis were carried out by using the Thermo Xcalibur software (version 2.2). Compounds were identified using the NIST Mass Spectral Library (National Institute of Standards and Technology, Washington DC, USA).

### S3.4 UV-vis analysis

A YOKE UV1901 diode array spectrophotometer utilizing a combination of a tungsten incandescent lamp and a deuterium lamp was used for UV-VIS absorption measurements. A 1 cm quartz cuvette was used for measuring absorbance and the deionized water was utilized as the spectroscopic blank. The detection range of the

entire spectrum was between 190-1100 nm.

S3.5 pH measurement

pH measurement was performed by a SX-610 pH-meter (Shanghai San-Xin) equipped with a SX615 combination glass electrode with saturated KCl as the inner reference solution, and calibrated with pH 4, 7, 10 standard buffers (Shanghai San-Xin).

# S3.6 Equilibrium calculation

All speciation calculations in this work were carried out with a chemical equilibrium calculation program-Visual MINTEQ at fixed  $NO_2^-$  concentration of 1mM at pH range from 2.0-5.0, 25 °C.

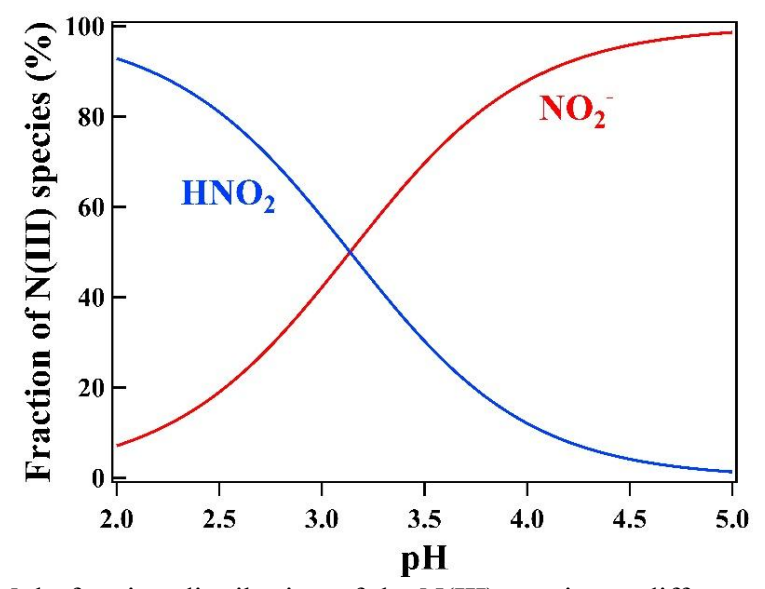


**Figure S1.** Mole-fraction distribution of the N(III) species at different pH values (25  $^{\circ}$ C, [NaNO<sub>2</sub>]<sub>0</sub> = 1 mM).

The fraction of •OH that reacts with NO<sub>2</sub> is determined as: 

$$Y_{OH}^{NO_{2}^{-}} = \frac{k_{NO_{2}^{-}}[NO_{2}^{-}]}{k_{NO_{2}^{-}}[NO_{2}^{-}] + k_{VL}[VL]} \times 100\% = 99.6\%$$
280
281 (1)

Where 
$$[NO_2^-] = 1 \times 10^{-3} \text{ M}, k_{NO_2^-} = 1.0 \times 10^{10} \text{ M}^{-1} \text{ s}^{-1}; [VL] = 1 \times 10^{-4} \text{ M},$$

283 
$$k_{VL} = 4.0 \times 10^8 \,\mathrm{M}^{-1} \,\mathrm{s}^{-1}.$$

The fraction of •OH that reacts with 2-propanol (2P) is determined as: 

$$Y_{OH}^{2P} = \frac{k_{2P}[2P]}{k_{2P}[2P] + k_{NO_2}[NO_2^-] + k_{VL}[VL]} \times 100\% = 99\%$$
 (2)

Where  $[2P] = 500 \times 10^{-3} \text{ M}$ ,  $k_{2P} = 1.9 \times 10^{9} \text{ M}^{-1} \text{ s}^{-1}$ ;  $[NO_2^-] = 1 \times 10^{-3}$ 

300 M, 
$$k_{NO_2^-} = 1.0 \times 10^{10} \,\mathrm{M}^{-1} \,\mathrm{s}^{-1}; \ [VL] = 1 \times 10^{-4} \,\mathrm{M}, \ k_{VL} = 4.0 \times 10^8 \,\mathrm{M}^{-1} \,\mathrm{s}^{-1}.$$

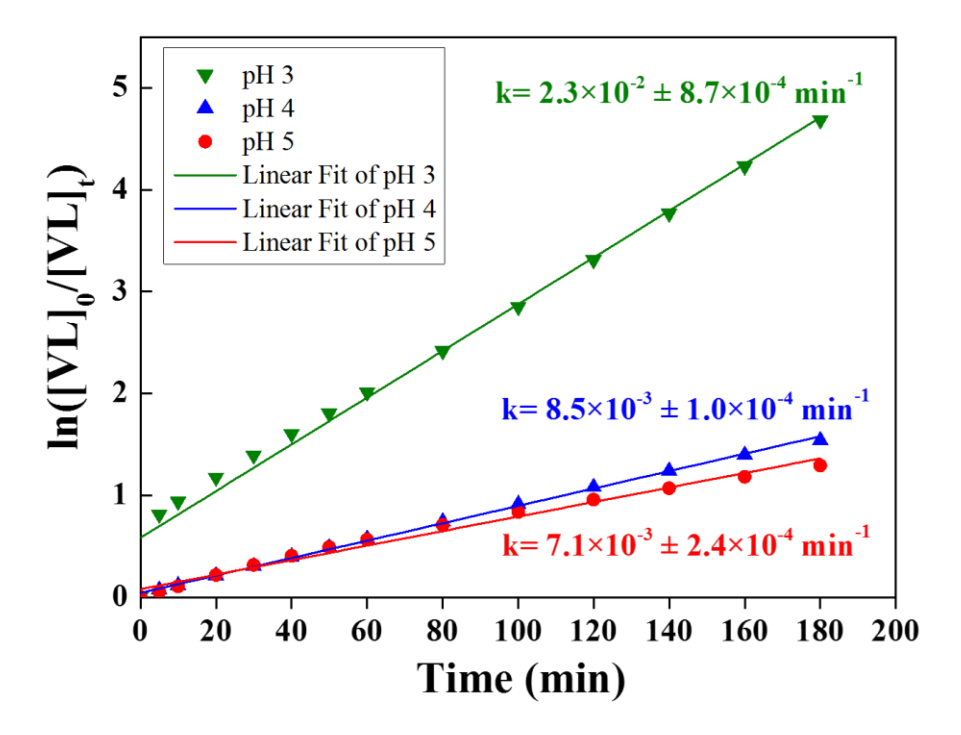


**Figure S2.** Effect of solution pH on the photooxidation kinetics of VL in the presence of nitrite.  $[VL]_0 = 100 \mu M$ ,  $[NaNO_2]_0 = 1 mM$ , air saturated solution.

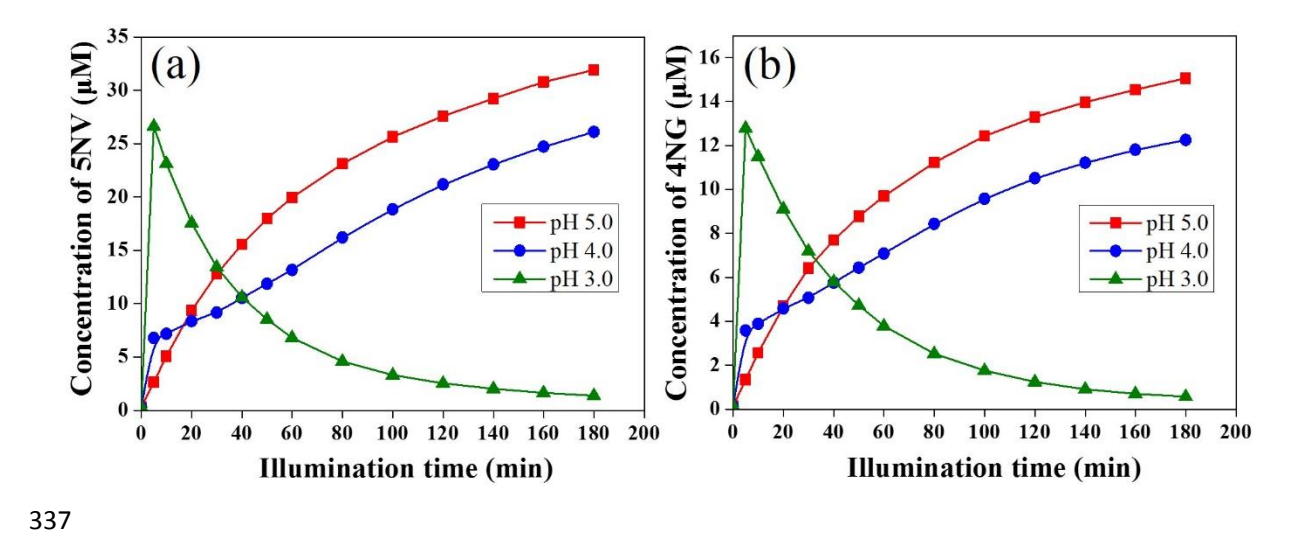


**Figure S3.** Effect of solution pH on the N(III)-mediated photoformation of 5-nitrovanillin (5NV) (a) and 4-nitroguaiacol (4NG) (b).  $[VL]_0 = 100 \mu M$ ,  $[NaNO_2]_0 = 1mM$ , air saturated solution.

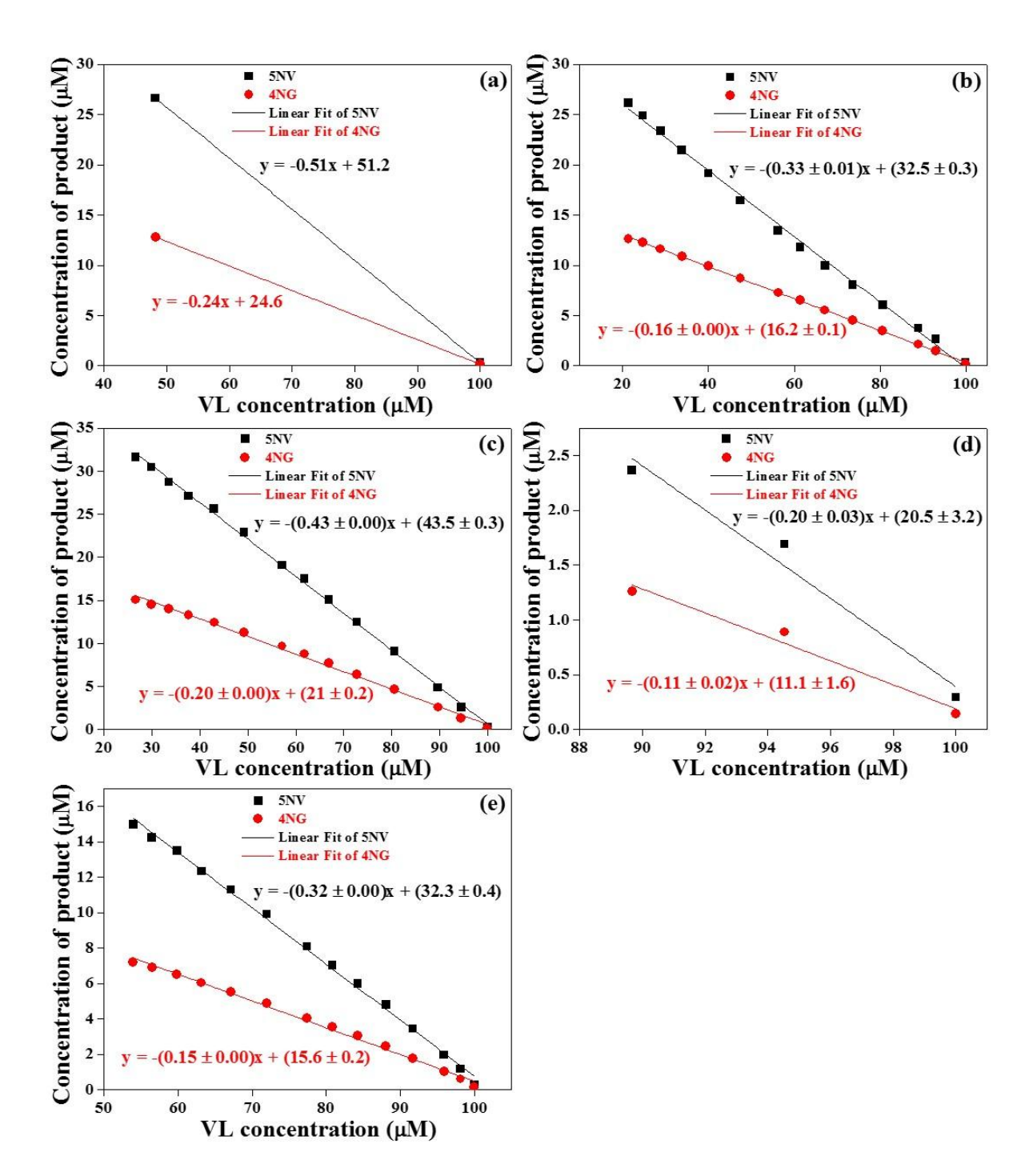
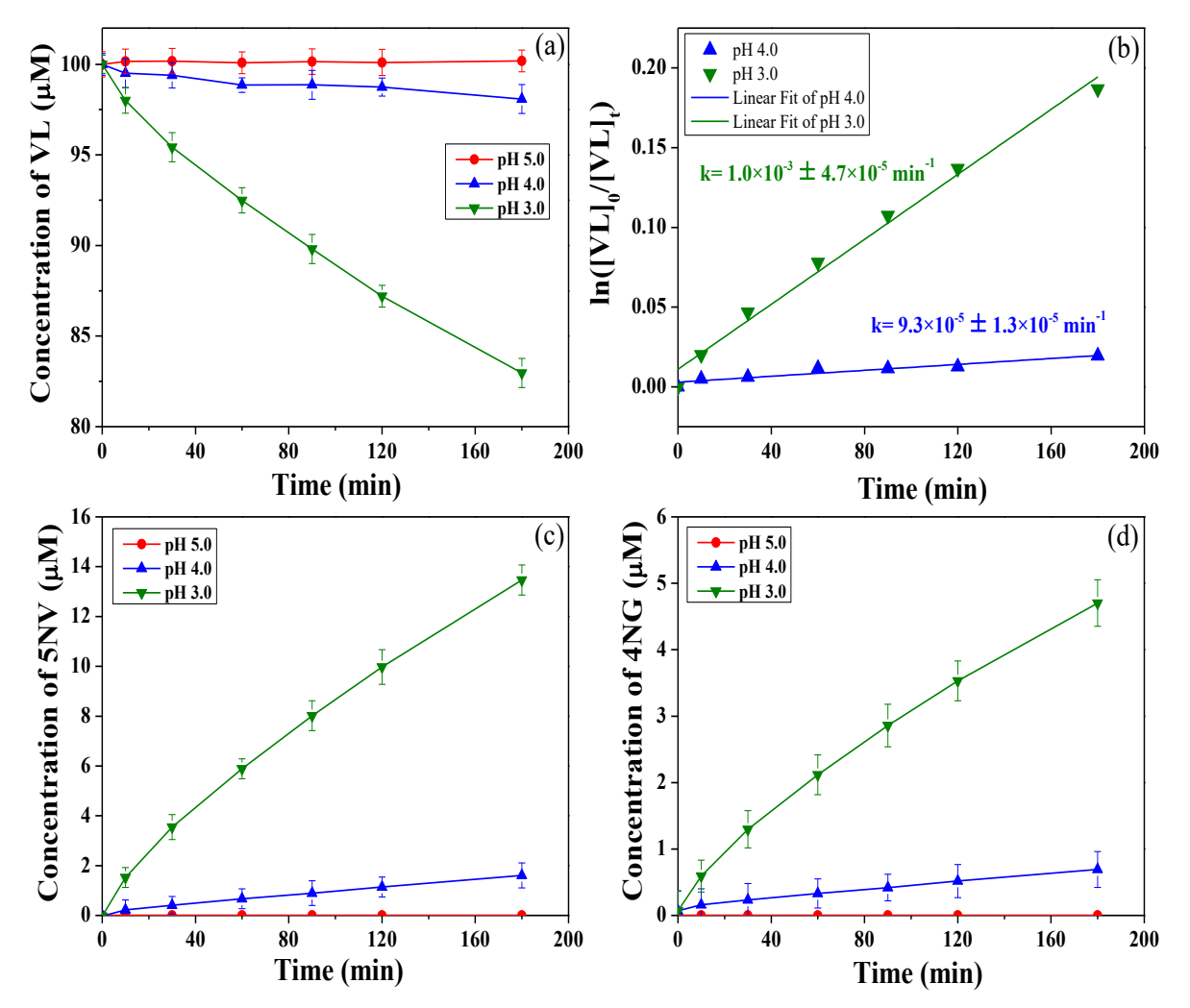
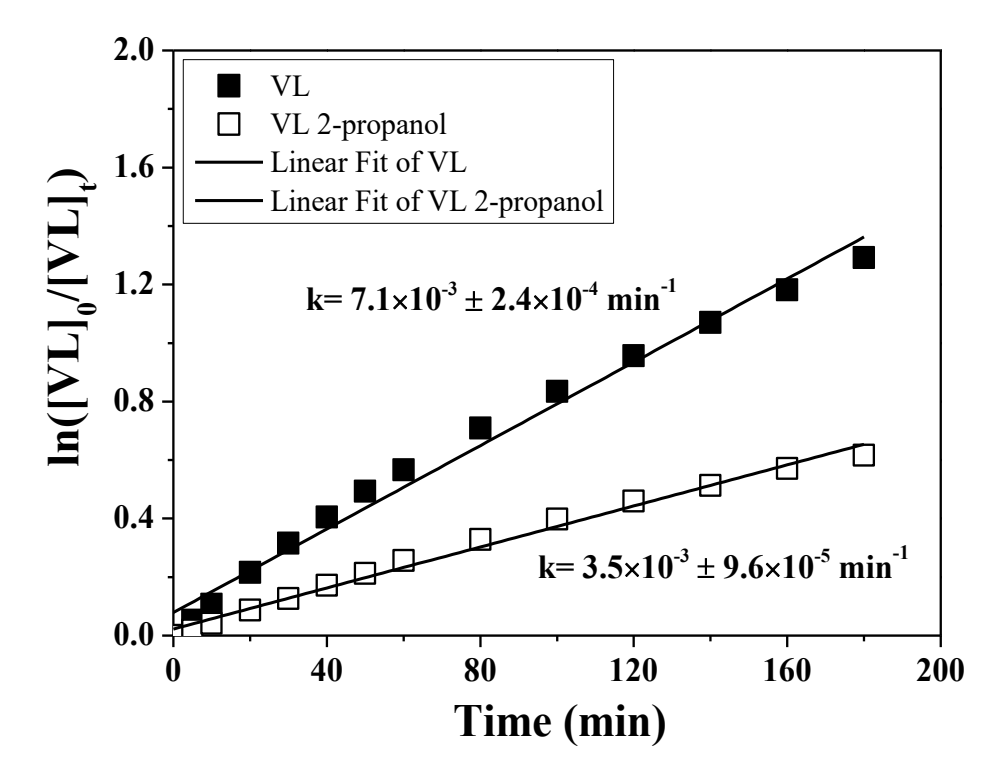


Figure **S4**. The yields of 5NV and 4NG from the photoreaction of VL with NO<sub>2</sub> under different experimental conditions. (a) pH=3, [VL]<sub>0</sub>=100  $\mu$ M, [NaNO<sub>2</sub>]<sub>0</sub>=1mM, air saturated solution. (b) pH=4, [VL]<sub>0</sub>=100  $\mu$ M, [NaNO<sub>2</sub>]<sub>0</sub>=1mM, air saturated solution. (c) pH=5, [VL]<sub>0</sub>=100  $\mu$ M, [NaNO<sub>2</sub>]<sub>0</sub>=1mM, air saturated solution. (d) pH=5, [VL]<sub>0</sub>=100  $\mu$ M, [NaNO<sub>2</sub>]<sub>0</sub>=1mM, N<sub>2</sub> saturated solution. (e) pH=5, [2-propanol]<sub>0</sub>=500 mM, [VL]<sub>0</sub>=100  $\mu$ M, [NaNO<sub>2</sub>]<sub>0</sub>=1 mM, air saturated solution. The absolute value of the slope for the line represents the yield of 5NV or 4NG.



**Figure S5.** (a) Effect of solution pH on the N(III)-mediated dark oxidation of VL. (b) Effect of solution pH on the dark-oxidation kinetics of VL in the presence of nitrite. (c) Effect of solution pH on the N(III)-mediated formation of 5-nitrovanillin (5NV) under dark condition. (d) Effect of solution pH on the N(III)-mediated formation of 4-nitroguaiacol (4NG) under dark condition. [VL] $_0 = 100 \, \mu M$ , [NaNO $_2$ ] $_0 = 1 \, mM$ , air saturated solution.



**Figure S6.** Effect of 2-propanol (500 mM) on the photooxidation kinetics of VL in the presence of nitrite.  $[VL]_0 = 100 \mu M$ ,  $[NaNO_2]_0 = 1 mM$ ,  $pH = 5.0 \pm 0.1$ , air bubbling.

No.	Retention time	Ion composition (m/z)	Proposed Structure	No.	Retention time	Ion composition (m/z)	Proposed structure
1	7.11 min	C <sub>9</sub> H <sub>7</sub> O <sub>5</sub> <sup>-</sup> (195.02997)	Unidentified	2	8.46 min	C <sub>8</sub> H <sub>6</sub> NO <sub>6</sub> (212.02011)	OH O2N OCH3 HO C>O
3	9.72 min	C <sub>8</sub> H <sub>6</sub> NO <sub>5</sub> <sup>-</sup> (196.02487)	OH O <sub>2</sub> N → OCH <sub>3</sub> H → C ⇒ O	4	10.12 min	C <sub>7</sub> H <sub>6</sub> NO <sub>4</sub> <sup>-</sup> (168.03005)	OH OCH <sub>3</sub> NO <sub>2</sub>
5	11.15 min	C <sub>14</sub> H <sub>9</sub> N <sub>2</sub> O <sub>6</sub> (301.04706)	Unidentified	6	12.74 min	C <sub>7</sub> H <sub>5</sub> N <sub>2</sub> O <sub>6</sub> (213.01522)	O <sub>2</sub> N OCH <sub>3</sub>
7	18.74 min	C <sub>15</sub> H <sub>12</sub> NO <sub>7</sub> (318.06195)	O <sub>2</sub> N OCH <sub>3</sub> OCH <sub>3</sub> OCH <sub>3</sub>				

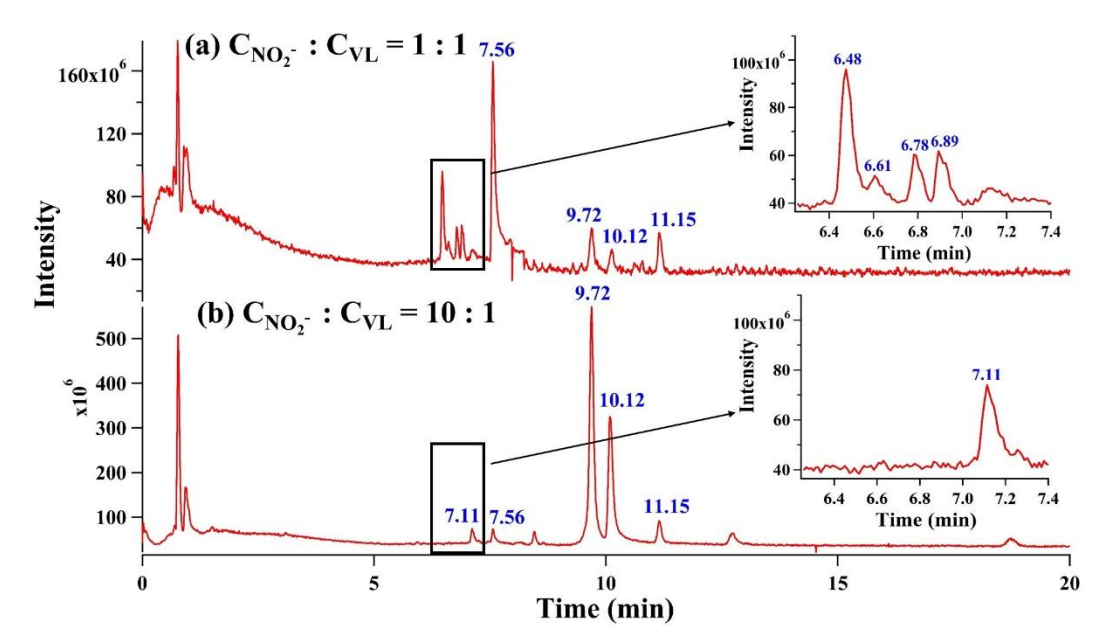


**Figure S7.** Total ion current (TIC) chromatogram for the sample taken from the photoreaction of vanillin (VL) with NaNO<sub>2</sub> at 180 min. (a). [VL]<sub>0</sub> = 100  $\mu$ M, [NaNO<sub>2</sub>]<sub>0</sub> = 100  $\mu$ M, pH= 5.0  $\pm$  0.1, air bubbling. (b). [VL]<sub>0</sub> = 100  $\mu$ M, [NaNO<sub>2</sub>]<sub>0</sub> = 1 mM, pH= 5.0  $\pm$  0.1, air bubbling.

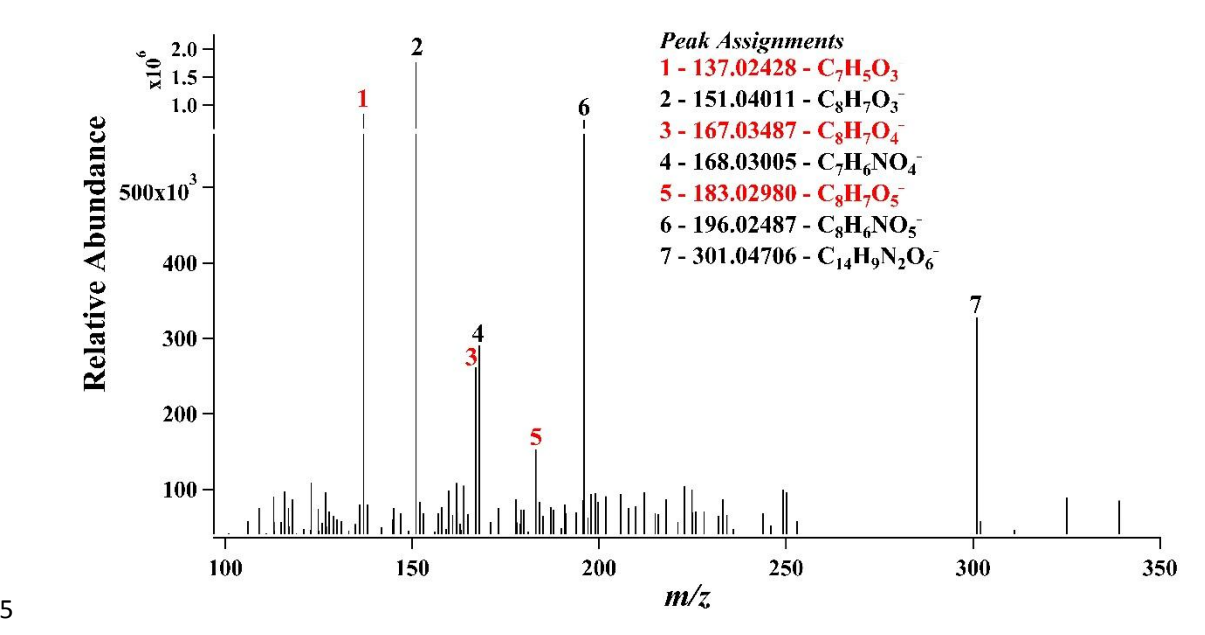


**Figure S8.** Average MS results for retention time 5-20 min of TIC chromatogram for the sample taken from the photoreactions of VL with NaNO<sub>2</sub> after 180 min. [VL]<sub>0</sub> =  $100 \ \mu\text{M}$ , [NaNO<sub>2</sub>]<sub>0</sub> =  $100 \ \mu\text{M}$ , pH =  $5.0 \pm 0.1$ , air bubbling.

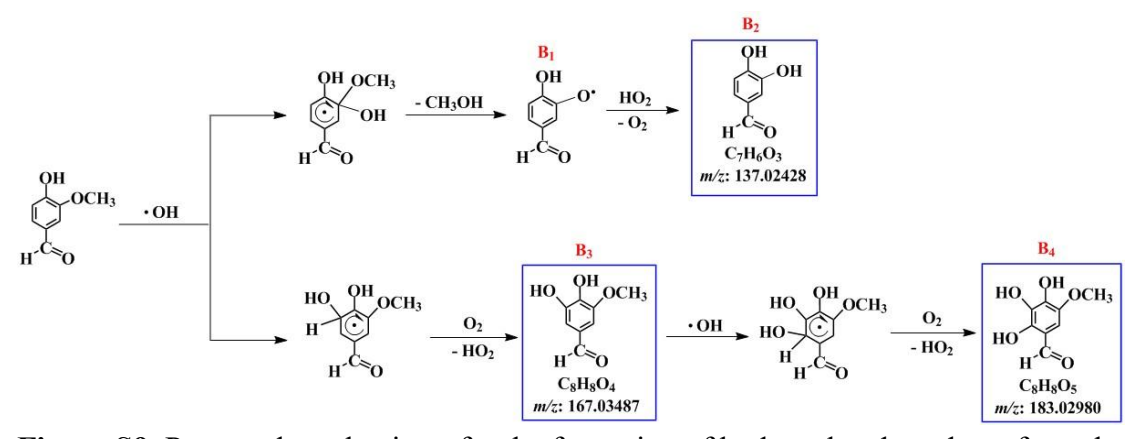


**Figure S9.** Proposed mechanisms for the formation of hydroxylated products from the photoreactions of VL with NaNO<sub>2</sub> after180 min. [VL]<sub>0</sub> = 100  $\mu$ M, [NaNO<sub>2</sub>]<sub>0</sub> = 100  $\mu$ M, pH = 5.0  $\pm$  0.1, air bubbling.

517 Unstable resonance structure

" delocalization arrow

**Figure S10**. The resonance structures for 5NV and 4NG at high and low solution pH, respectively. Structure I, III and V represent the most stable resonance struture when the corresponding compound is deprotonated. Structure II, IV and VI represent unstable resonance struture when the corresponding compound exists in its undissociated form.

Figure S11. The resonance structures for VL at high and low solution pH, respectively. Structure VII represent the most stable resonance struture when VL is deprotonated. Structure VIII represent unstable resonance struture when VL exists in its undissociated form.

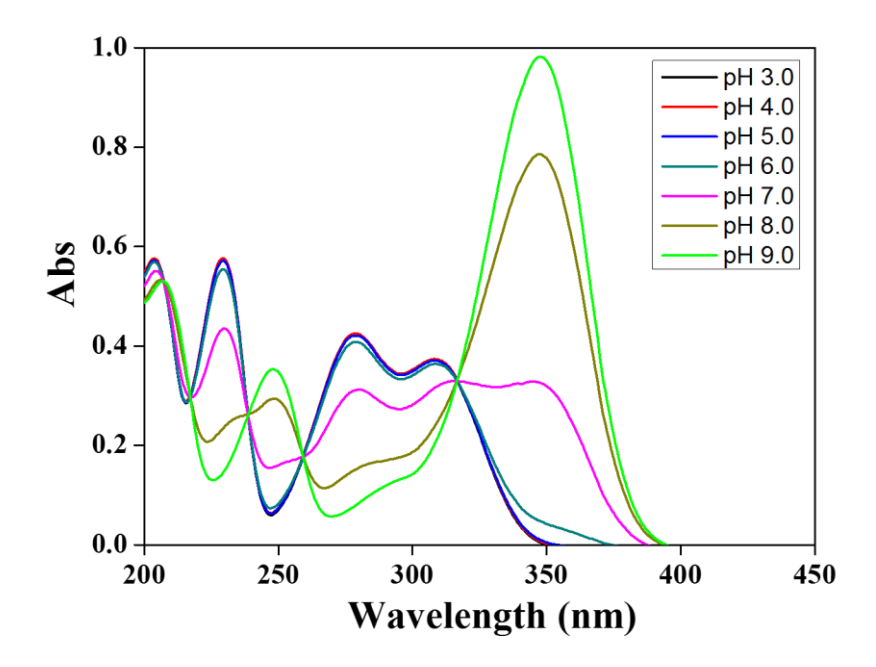


Figure S12. The UV-vis absorption spectra as a function of pH for 40  $\mu M$  VL.

552